CURJ

WINTER 2007
VOL.6 NO.2
CALTECH UNDERGRADUATE RESEARCH JOURNAL

TRACING CONNECTIONS IN THE GORILLA BRAIN

DW-MRI elucidates the gorilla brain's fiber organization.

DESIGN AS RESEARCH

A process description for the use of design as research.

Art Center College of Design

A leader in art and design education, Art Center challenges students through a transdisciplinary curriculum that embraces change and explores design-based solutions to real-world issues.

UNDERGRADUATE PROGRAMS

Advertising
Environmental Design
Film
Fine Art Media
Graphic Design
Illustration
Photography and Imaging
Product Design
Transportation Design

GRADUATE PROGRAMS

Art
Criticism and Theory
21st Century Cinema
Industrial Design
Media Design

CURJ IS A COLLABORATIVE EFFORT BY STUDENTS AT ART CENTER COLLEGE OF DESIGN AND THE CALIFORNIA INSTITUTE OF TECHNOLOGY.

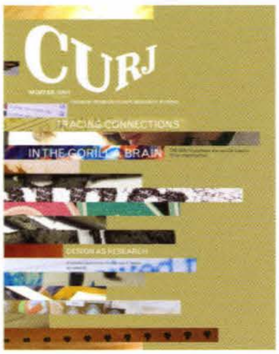

Be BIOMEDICAL ENGINEERING

Ee ELECTRICAL ENGINEERING

Ss SOCIAL SCIENCE

Ph PHYSICAL SCIENCE

Bi BIOLOGY

INTERVIEW

RESEARCH

FINIS

CALTECH UNDERGRADUATE RESEARCH JOURNAL VOL. VI NO. II

● Art Center College of Design

FROM THE EDITOR

"The most beautiful thing we can experience is the mysterious. It is the source of all art and science. He to whom this emotion is a stranger, who can no longer pause to wonder and stand to rapt in awe, is as good as dead...his eyes are closed." -Albert Einstein

How often have we looked out into the cosmos and not felt the weight and awe of the vast unknown? When was the last time we didn't feel that spark of amazement when looking under the microscope to discover whole new complexities to the smallest fragments of life?

These life mysteries that constantly surround us in wonderment are what drive scientists to conduct great research and pursue hard to grasp answers. That curiosity keeps us up at night for those extra few hours and from time to time provides us with the means towards revelations that change the world we live in. Just as Dr. Goodstein further analyzed the 2007 oil predictions to predict one of the world's most imminent crises, undergraduates also get the chance to pursue mysteries of their own. From understanding the day to day moral judgments we continually face to mapping the intricate networks of the brain, these questions drive undergraduates to go beyond standing in awe of mysteries to discovering their truths.

The Caltech Undergraduate Research Journal is a showcase of the great work that undergraduate scientists carry out. It is the acknowledgment that great research starts from a passion for the mysterious whether it is purely scientific or simply a question about human behavior; it is the need to open our eyes to the vast possibilities of our world whether we are professors in academia, undergraduates finding our own truths, or even a 10-year old who just received their first magnifying glass. Never stop being amazed, never stop asking questions.

Helen Lee
Editor-in-Chief

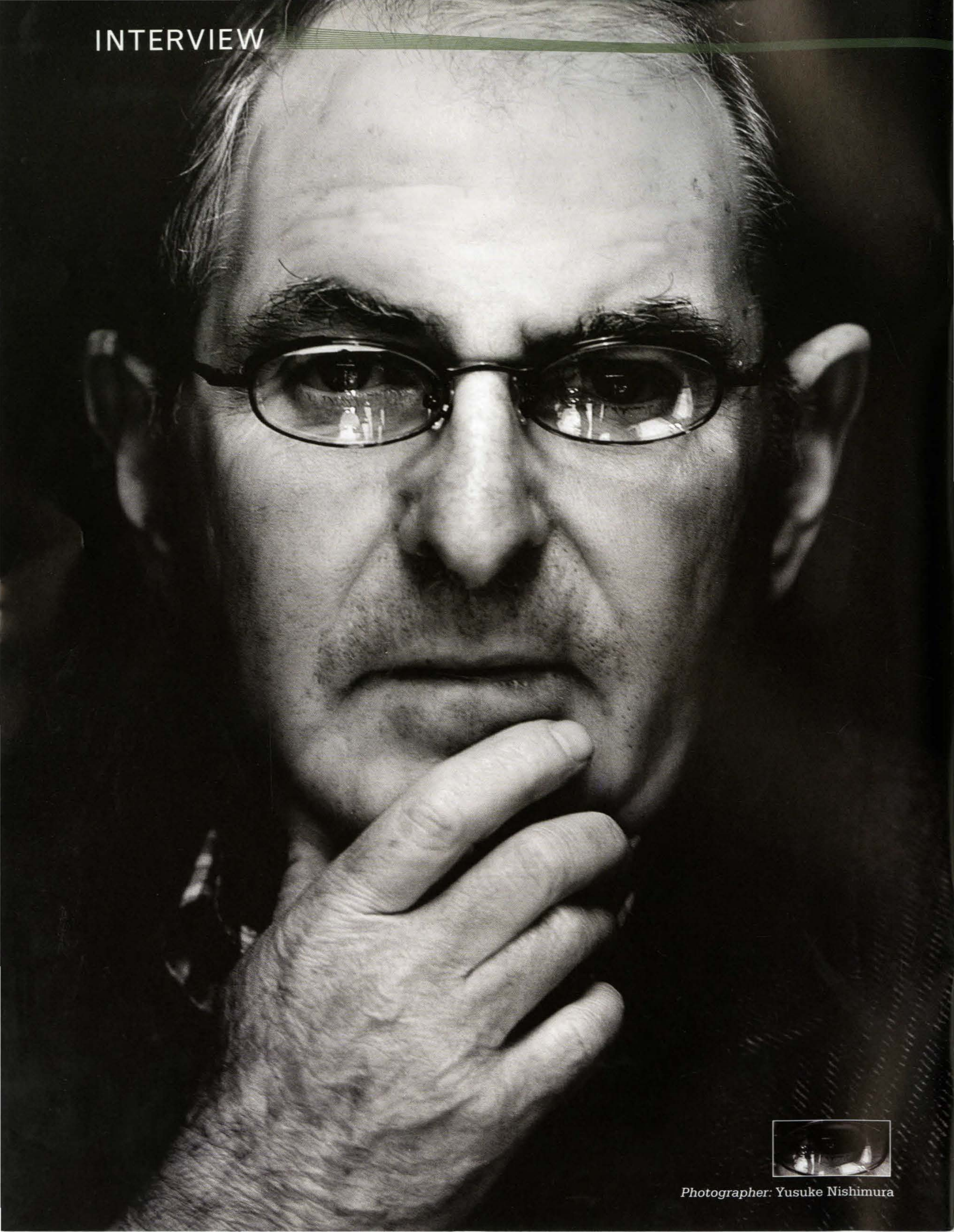

Photographer: Yusuke Nishimura

INTRODUCTION

Dr. David L. Goodstein, Ph.D. is a well-established scientist, a prominent and respected researcher in the many areas of Condensed Matter Physics, a field that he himself was a pioneer of.

AMAZINGLY ENOUGH, THE ENTIRETY OF HIS RESEARCH has allowed him to write close to 200 publications. He is currently the Vice Provost at Caltech, a place where he has been teaching for forty years; in 1995, he was even made the Frank J. Gilloon Distinguished Teaching and Service Professor. In his time, he has produced many widely used educational products including *The Mechanical Universe*, a 52-part telecourse for college students, which later was modified for high school use as well. One of his more recent interests is the energy crisis, a crisis that when he originally delved into, no one cared about. However, now even the most popular attractions at Disney World in Orlando, Florida feature the crisis as one of the main educational themes to the millions of families that visit. Another of his concerns in science and society is conduct and misconduct. In this he has also been very successful. When asked, he describes Caltech as "a great place, a wonderful place to teach, where the students are excellent, the facilities are excellent, and everything's excellent."

INTERVIEW

Q: *According to* Physics Today, *you "created" Condensed Matter Physics. How do you feel about that? Can you give us a brief description of what it is and how it is important to us?*

A: Well, I feel very good about it. And, I didn't create Condensed Matter Physics, but I did write a textbook about it. Condensed Matter Physics isn't just the study of all condensed matter, of matter and molecules, but of condensed matter, solid matter, superconductivity, superfluidity, and all kinds of magnetic phenomena in various materials. It's a very lively field.

Q: *How did you get involved in the research field? Were there specific events in your childhood that led you to academia?*

A: No, my interest started while I was in college. When I received my first 'A', I looked at my instructor and said "That's the life of me".

Q: *You seem to have done a lot of research dealing with phases and phase transitions in topics such as: adsorbed, two-dimensional matter, ballistic phonons in solids, superfluidity in liquid helium, critical point phenomena, and now the dynamics of the superfluid phase transition in the absence of gravity. How was working in all these fields different, and what was the most enjoyable?*

A: It was all enjoyable. There isn't one that I can pick out and say it was most enjoyable. All these fields were very interesting. The ideas just came upon me. I would be minding my own business, and somebody would come and suggest that I do this or that.

Q: *Of late, you are focusing more on science and society, looking at conduct and misconduct in science, the end of exponential growth of the scientific enterprise, and the energy crisis as described in your most recent book,* Out of Gas. *How and why did you become interested in this?*

A: Well, I've always been interested in science and society. As for the energy crisis – on June 11, 2001, just three months before September 11, I was reading the LA times, and I saw a story; it had a graphic that showed one of the predictions of oil in 2007. It was a catastrophe. I said to myself, 'That's a prediction of what oil will be like in six years, I need to find out what this is all about.' So I started to look into it and eventually *Out of Gas* came about.

Q: *As I read in* Out of Gas, *the energy crisis is most imminent. In this very complicated situation, what do you think is the best way to get people's attention towards this matter?*

A: When I wrote the book three years ago, nobody was paying any attention. Now it's on the front burner for everybody; it's become a part of natural discourse. Even the president mentioned it in his State of the Union Address. So I think people are becoming aware of this very rapidly, and that's a good thing.

Q: *What can most everyday people do to help alleviate the condition instead of just sitting, waiting, and hoping someone else will solve the problem for them?*

A: They can conserve fuel – that means driving hybrid cars and making their homes more energy efficient. They can do all sorts of things to conserve fuel, because that's where the crunch is, fuel.

Q: *In* Out of Gas, *you talked about class demos including one demonstrating the conservation of energy where you would pull a bowling ball towards your face. Once the ball touched your face you would let go and watch the ball swing back and forth, to and fro, within inches from your face as it confirmed the eternal law, knowing that as long as the ball had conserved energy, it would not hit you. However, have you ever accidentally leaned forward?*

A: No, I put a bar up behind my head and I keep my head against the bar, as a constant reminder to myself not to lean forward.

Q: *Do you think you are going to write more books in the future?*

A: Oh I might. But after you've written a book about the end of civilizations, it's very hard to write another.

"...my interest started while I was in college. When I received my first 'A', I looked at my instructor and said 'That's the life of me.'"

Q: *Another one of the things you are involved in is misconduct in science. Can you tell us more about that?*

A: Yeah. There was a very high profile case at Caltech in the laboratory of Lee Hood some years ago. This alerted us all to the problem. At that time, I had written regulations for Caltech that became Caltech's regulations on misconduct. The government honed in on the situation; however, their own regulations on misconduct were objectionable. They were not as good as ours. So I kept ours in place and ignored the government's until I got a letter from them saying 'Change your regulations, or else!' They gave me 90 days to reply. I waited 89 days and responded that it takes time to change things in a university – you have to hold committees to consider the changes first. I got an answer back saying 'Alright, send us your new rules when you have them.' I took that to mean there was no pressure at all, because "when we have them" is not a deadline. That being the case, I ignored the government.

Eventually, the government adopted really good rules – more or less like ours – and we adopted the government's rules, and so that was very successful. Unfortunately, during this period there were two occasions when two young people came to me for advice. The committees had gotten all upset because someone had accused them of misconduct. Thankfully, on both cases I was able to say very specifically that by the Caltech rules, what they were accused of was not misconduct. Their actions could perhaps on the federal rules have been labeled as misconduct, but the federal rules were very vague and very general. In spite of this, both the young scientists are among our brightest stars today, so I think I did a good job.

Q: *What is a memorable story you can tell us – perhaps of something that happened in class, in lab, or in a seminar?*

A: One of the Houses used to have a special day where they would serve pizza in class. I put a stop to that because I thought the other students deserved better.

Q: *Have you ever had any really crazy research ideas that ended up not working out?*

A: Oh sure, there have been research projects that lead nowhere. Then I gave up and went onto something else.

Q: *What are some future projects you would like to work on?*

A: Well, I would like to write more books. But as I say, I have the problem of writing a book after I've written a book about the end of civilization. □

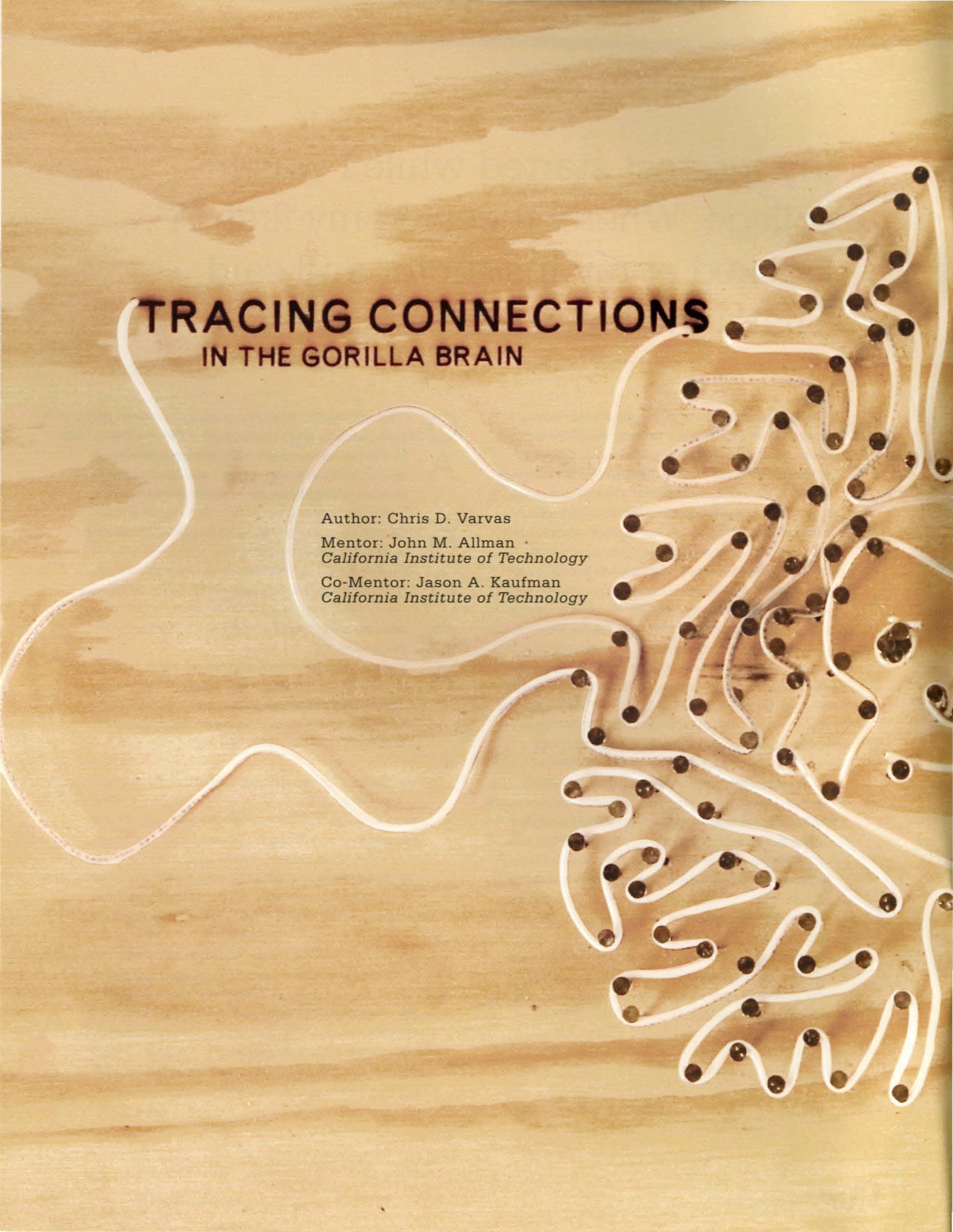

TRACING CONNECTIONS
IN THE GORILLA BRAIN

Author: Chris D. Varvas

Mentor: John M. Allman
California Institute of Technology

Co-Mentor: Jason A. Kaufman
California Institute of Technology

WHEN READING WORDS ON A PAGE, WE OFTEN take for granted that part of ourselves which plays a key role in enabling the action of reading—the brain. Yet the specific connectivity of brain structures permits the reader to delight in the task of reading. A person's reading skill is encoded in some of those neural pathways. Therefore, differences in connectivity account for variance in reading ability between people. Additionally, non-musicians can be distinguished from musicians based on comparing neural pathways. The capacity for literacy, both with words and with musical notes, is regarded as a higher cognitive function that is not entirely understood.

Quantification of regional connectivity is vital to understanding how the brain functions, but until recently, technology has not been used to measure the connectivity in humans and great apes. Connectivity mediates the sources of input information available to a region of the brain in addition to influencing the destinations of output information. A comparison between the connectivity of great apes (gorillas, gibbons, orangutans, and chimpanzees) and humans will help scientists understand the anatomical underpinnings of uniquely human cognitive abilities. However, since there are no direct data on regional brain connectivity in great apes and humans, these data must be inferred from macaques, the closest relative whose neural connectivity has already been studied. Because the traditional methods of using neuronal tracers are terminal, ethical limitations prohibit tract-tracing studies from being conducted on great apes and humans. Another drawback of this invasive method is that it reveals only a restricted number of small fiber tracts because small injection sites are used. Other post-mortem techniques, such as carbocyanine dyes and degeneration studies, have at least provided some direct information on human brain connectivity. Unfortunately, carbocyanine dyes are constrained by very slow diffusion rates and are therefore impractical for tracing long-distance connections. Degeneration studies are limited by the chance nature of brain lesions. Therefore, the information gathered from human brain studies has been limited in scope.

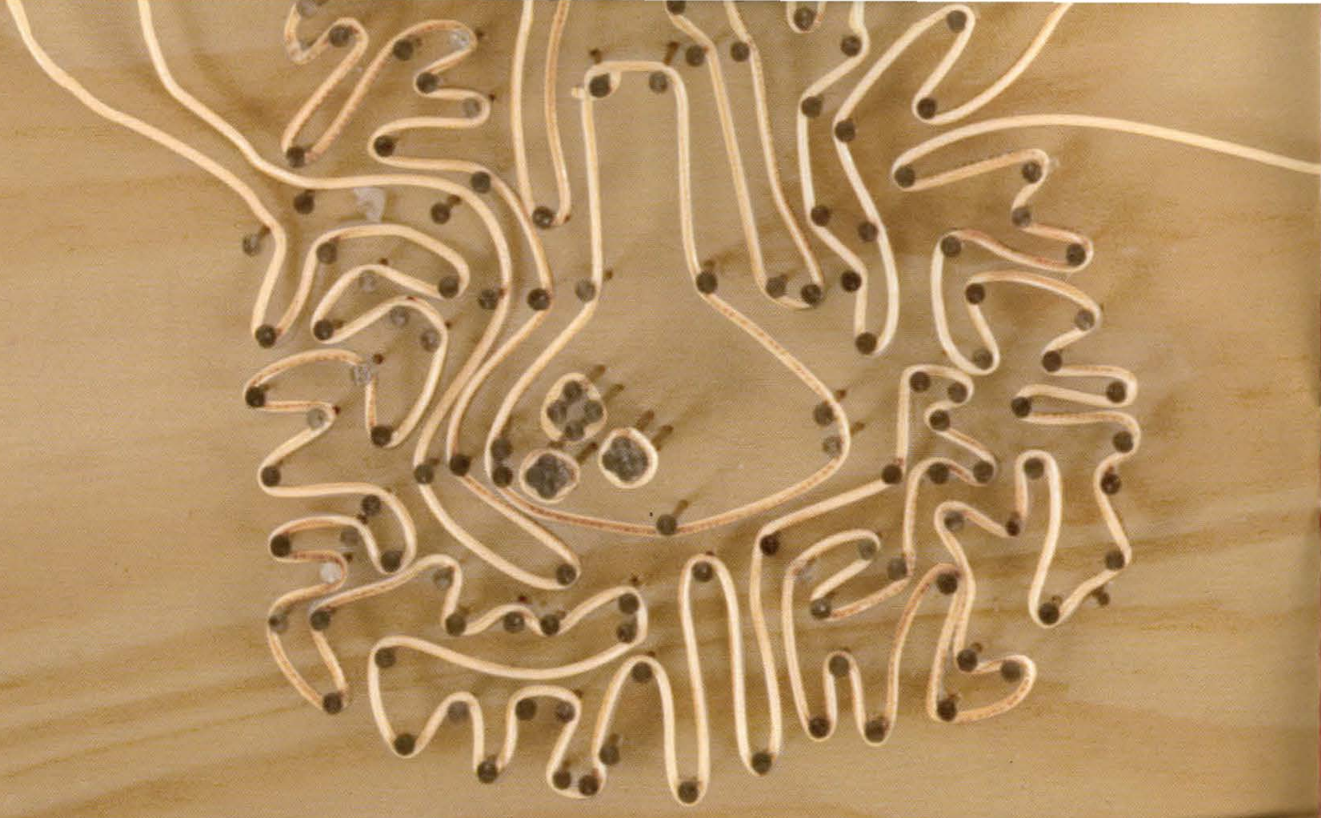

Although previous techniques for looking at brain connectivity were too invasive and incomplete to develop a full understanding, a new method called diffusion-weighted magnetic resonance imaging (DW-MRI) may be more useful in elucidating the brain's fiber organization.

NEW TECHNOLOGY TO MEASURE BRAIN CONNECTIVITY

Diffusion-weighted MRI (DW-MRI) is a recently developed, non-invasive technique, which is used to measure brain connectivity and can be performed on living subjects as well as post-mortem tissue. DW-MRI is a variant of magnetic resonance imaging that is sensitive to the Brownian, or random, motion of water molecules. In tissue that has a high degree of directional order, also called anisotropy, water preferentially diffuses parallel to that major axis.

In brain white matter, tracts of axon bundles are highly anisotropic: water molecules preferentially diffuse along axon tracts and perpendicular motion is restricted. DW-MRI measures both the primary orientation and the degree of anisotropy of Brownian motion within each voxel, or volume element. As such, DW-MRI can be used to infer the organization of the axon bundles. Since DW-MRI is non-invasive, it can be performed on living humans and great apes. Another significant benefit of DW-MRI is that it gives a global data set of the whole brain's fiber organization; in contrast to traditional tract-tracing methods, it is not limited to few fiber tracts. Thus, DW-MRI allows for examination of connectivity in any region of the data volume.

Recent advances in DW-MRI have resulted in more accurate measurements. A new DW-MRI technique called "high angular resolution diffusion imaging" (HARDI) has improved upon the older diffusion tensor imaging (DTI). While DTI incorporates diffusion measurements in six directions, HARDI uses as many as twenty directions or more, contributing to higher resolution images. After diffusion data is collected in the form of a 3D vector field, one of several methods of tractography must be employed to reconstruct the fiber tracts. Reconstruction of the tracts has inherent error because connectivity must be inferred from voxel to voxel. Even so, tractography methods that process data collected by HARDI are more accurate and advanced than those collected by DTI. DTI data can only be processed by maximum-likelihood approaches, like "fast marching tractography" (FMT). A major limitation of maximum-likelihood approaches is that they must take anisotropy into account. The result is that their tracts terminate prematurely near gray matter due to its low anisotropy. HARDI allows for a more advanced form of tractography called "probabilistic fiber tractography" (PFT), which reconstructs all possible tracts from a specified region and calculates the probability of each pathway. Thus, it quantifies the uncertainty of pathways. This is an improvement over maximum-likelihood approaches, which do not calculate the probabilities of the tracts. Another advantage is that PFT eliminates the need for anisotropy information, allowing for tract-tracing near and into gray matter. Rather than relying on anisotropy information, it utilizes diffusion orientation. Furthermore, PFT is resistant to noise, otherwise known as the mistaken measurement of a voxel's primary orientation. Such noisy voxels usually send tracts on errant routes. Since tracts with errant routes generally have low probability, experimenters using PFT can distinguish these easily.

FIGURE 1

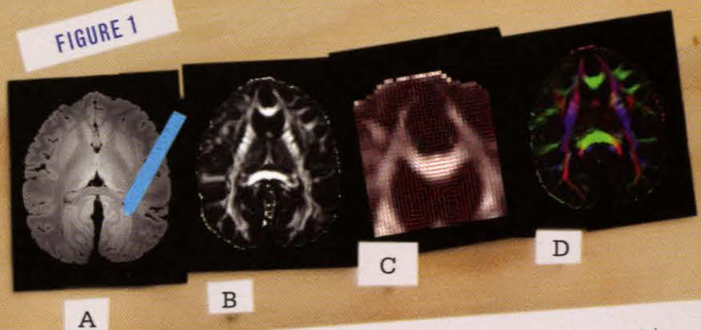

Results of the anatomical and DW-MRI scans in approximately the same axial section. (A) Anatomical MRI scan. The Stria of Gennari can be seen in primary visual cortex (arrow). (B) Anisotropy in each voxel; brighter areas have higher anisotropy. The internal capsules (IC), the splenium (CCspl), and genu (CCgenu) of the CC have high anisotropy. (C) Primary diffusion direction in each voxel represented by lines, superimposed on the anisotropy profile. Shorter lines signify that fibers are oriented away from the axial plane. Section is centered on the callosal genu. (D) Color-coded representation of primary diffusion direction in each voxel. Green denotes a left-right direction; red is anterior-posterior; and blue is inferior-superior. Intermediate directions have mixed colors. The image is modulated so that the color brightness is proportional to the anisotropy value. The posterior part of the corona radiata (CRp) is oriented anterior-posterior.

BRAIN CONNECTIVITY STUDIED DIRECTLY IN *GORILLA GORILLA*

Our study used DW-MRI in the first connectivity analysis of *Gorilla gorilla*. Specifically, we examined the organization of cortical fibers crossing the corpus callosum (CC) and fibers of the corticospinal tract. The CC is the primary bridge between the hemispheres. The corticospinal tract carries motor instructions to the rest of the body,descending from the primary motor cortex (M1). We chose to study the CC's connectivity profile and the coticospinal tract in part because we could compare our results to previous DW-MRI studies that analyzed these same regions. Rather than working with living subjects, we performed the scans on a fixed, isolated gorilla brain in an experimental MRI system with much greater resolution than clinical MRI. FDA regulations prohibit scans of living subjects in magnetic field strengths greater than 3.0 Tesla. Studying a fixed brain allowed us to use an MRI system with a high magnetic field strength of 9.4 Tesla, which yields greater image resolution. Another advantage of using a fixed brain was that it enabled us to perform scans for extended time periods, which increased the signal to noise ratio and thus improved the quality of data obtained. Additionally, use of a fixed brain permitted us to perform histology following the scans. The details gained from histological information provided more accurate connectivity results.

The high-field MRI scans of the formalin-preserved *Gorilla gorilla* brain yielded structural brain images with four to six times the resolution of conventional MRI done with clinical scanners [Figure 1a]. Using the 9.4 Tesla system, we were able to achieve an isotropic voxel size of 250 microns. These structural images reveal brain anatomy that had not been previously visible in MR imaging, including feathering of the lenticulostriate bridges and the presence of the Stria of Gennari in primary visual cortex. For the diffusion scans, we were able to achieve an isotropic voxel size of 1mm, which is more than twice the resolution of even the most sophisticated diffusion spectrum scans thus far published.

The results of the scans were consistent with our expectations. For example, high anisotropy was observed in white matter structures, such as the internal capsules and the splenium and genu of the CC, and low anisotropy was observed in gray matter, such as the cortex [Figure 1b]. Next, in areas of high anisotropy, there was a high degree of order with respect to the primary diffusion direction. For example, voxels of the callosal genu were highly anisotropic and their primary diffusion orientations were streamlined; in contrast, the gray matter structures had little directional order [Figure 1c]. Lastly, the observed fiber directions were as expected; for example, the fibers of the posterior part of the corona radiata were oriented anterior-posterior [Figure 1d].

FIGURE 2

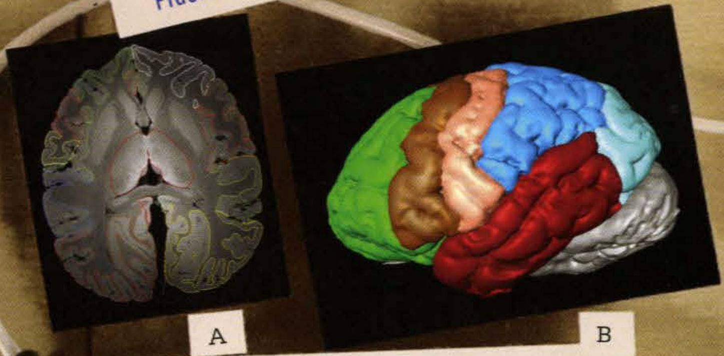

Results of anatomical MRI segmentation. (A) Axial slice manually segmented in the program. Each slice combined to give the 3D image in (B). Included is the frontal lobe (green), precentral gyrus including M1 (brown), somatosensory cortex (pink), parietal lobe (blue), occipital lobe (light blue), and temporal lobe (red). Non-parcellated tissue is gray. The colors do not match those in the 2D slice.

FIGURE 3

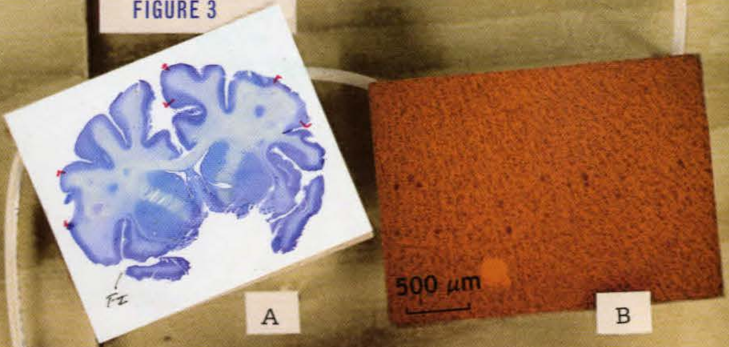

Histological section used to refine segmentation of M1. (A) Nissl-stained histological section. (B) Histological section magnified at 400x. The larger, pyramidal cells are Betz cells, which indicate M1. The slide in (A) was marked in red according to their location, and that information was used in the segmentation.

Once the raw MRI data was collected, we had to parcellate the brain into regions-of-interest in order to perform PFT. Manual segmentation of the anatomical MRI image one slice at time [Figure 2a] produced 3D regions [Figure 2b]. PFT was conducted on the diffusion data following segmentation. In examining the connectivity of the CC, we asked the following question: Which cortical region does each voxel in this segmented region connect to? In examining the corticospinal tract, we calculated the probability of all tracts connecting to M1, and we limited the results to tracts that also passed through a waypoint region, the internal capsule. The voxel coordinates of the regions-of-interest were obtained from the anatomical MRI segments.

The cortex was the first region to be parcellated. It was segmented according to morphological boundaries in which the cortical sulci, or grooves, were used to divide the lobes and functional subdivisions within the lobes. The CC was then segmented, creating one of the two regions analyzed for connectivity, called "seed regions." The CC was also parcellated according to morphological boundaries. Segmentation of M1, the second seed region, was uniquely based on histology, which represents functional regions more accurately than gross morphology. This involved studying the microstructure of the stained brain tissue. The presence of Betz cells, which are large, layer V pyramidal neurons, defined the borders of M1 [Figure 3a,b]. This information was then transferred from each histological slide to its matching anatomical MRI slice in order to create the M1 seed region.

Using a waypoint region allowed us to limit our results to only the corticospinal tract since it is the only tract that connects to M1 and passes through the internal capsule. We defined our waypoint region as the part of the internal capsule that contains corticospinal tract fibers, and this subdivision was identified using PFT. To do so, we first segmented a seed region of the entire internal capsule based on morphology [Figure 4a]. Then, we examined its connectivity profile using PFT, looking at which cortical region each voxel in this seed region connected to [Figure 4b]. The subdivision of the internal capsule that had the highest probability of connectivity to M1 was then labeled as the waypoint region [Figure 4c].

OBSERVATIONS CONFIRMING EXPECTATIONS

The results of our CC analysis were consistent with previously reported data. One similar finding was the predominance of frontal lobe fibers. In our study, frontal cortex fibers composed about 47% of the anterior CC [Figure 5]. In their study of human CC, Hofer and Frahm (2006) found that about 55% of the anterior CC was composed of frontal cortex fibers [Figure 6a]. Huang et al. (2005), also studying humans, calculated that the anterior 66% of the CC was composed of frontal cortex and M1 fibers; our study found the value to be 66% as well. [Figure 6b] All of these percentages are rough approximations.

We hypothesize that the gorilla showed less connectivity between the CC and the frontal lobe because gorillas have a smaller frontal lobe than humans. The predominance of frontal lobe fibers to the CC (relative to the size of the frontal lobe itself) for both the gorilla and humans can be explained by the fact that the frontal lobe consists mainly of association cortex and not of primary or secondary sensory/motor cortex. In essence, the frontal

FIGURE 4

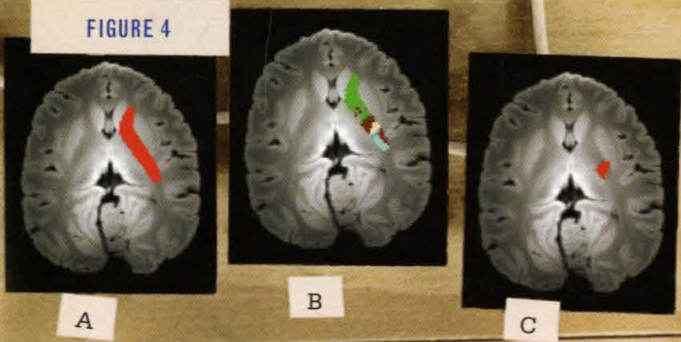

Segmentation of waypoint region for corticospinal tract analysis in axial section. (A) Morphologically-based segmentation of entire right internal capsule. (B) Most probable cortical connections of internal capsule voxels obtained using PFT. (C) Waypoint region created from subdivision of internal capsule that had the highest probability of connectivity to M1.

FIGURE 6

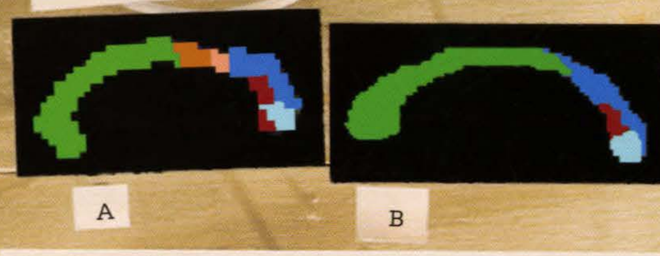

Most probable connections of CC voxels near the midline in sagittal sections observed by (A) Hofer and Frahm (2006) and (B) Huang et al. (2005). Unlike Hofer and Frahm and ourselves, Huang et al. did not differentiate (through segmentation) the precentral gyrus from the rest of the frontal lobe, and they did not differentiate the somatosensory cortex from the rest of the parietal lobe.

FIGURE 5

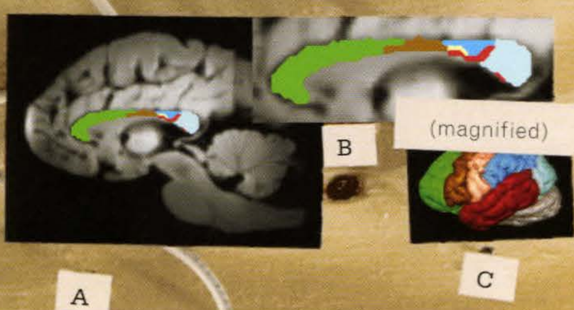

Most probable connections of CC voxels near the midline in sagittal section. Possible cortical connections include the frontal lobe (green), precentral gyrus (brown), somatosensory cortex (pink), parietal lobe (blue), occipital lobe (light blue), and temporal lobe (red). (B) is a magnified version of (A) and (C) is a figure legend.

lobe serves executive functions in the brain and so it needs to connect to many areas, including areas in the opposite hemisphere, and the CC is the primary bridge between hemispheres. We would not expect that pattern in primary or secondary sensory/motor cortices since they only process information locally and then pass that information to the next level in the hierarchy. Frontal cortex is at the very top of the hierarchy, so it connects to many areas of the brain.

Another similarity to past experiments was the order of fiber-types through the CC. From anterior to posterior, we found the CC fiber-types to be in the following order: frontal lobe, PCG, somatosensory cortex, parietal lobe, and occipital lobe, with the temporal lobe on the posterior, ventral surface [Figure 5, 6a,b]. The ordering makes sense because the cortex has the same order anterior to posterior, and this indicates that the front of the CC is indeed connected to the front of the cortex. Another consistent finding was that the different fiber regions of the CC were segregated.

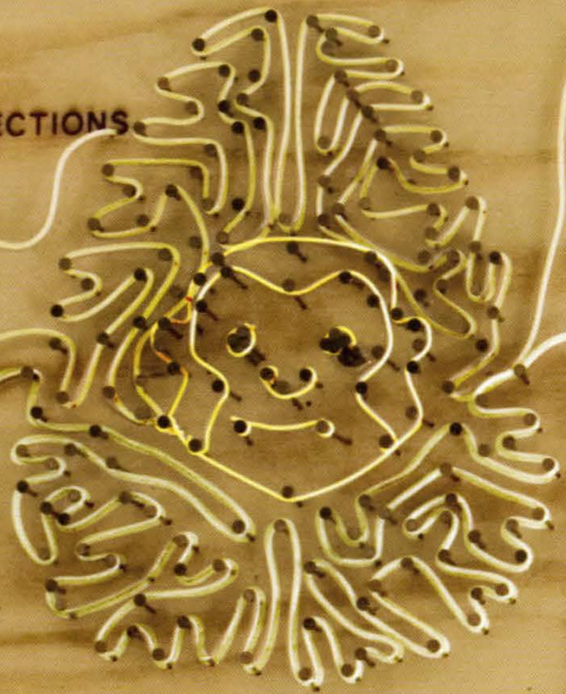

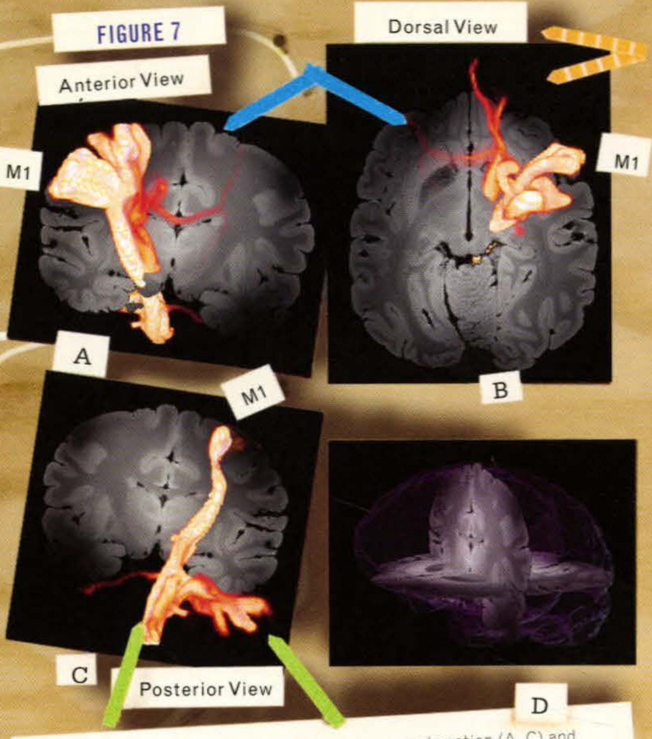

Results of the corticospinal tract analysis in coronal section (A, C) and axial section (B). Primary motor cortex (M1) was the seed region and the internal capsule was the waypoint region. Projections descended from M1, through the posterior limb of the internal capsule, then through the cerebral peduncle, and down to the pyramids of the spinal column. Projections to the cerebellum were also found (green arrows). Additionally, minor projections were detected from the motor portion of the thalamus that connect to areas of the prefrontal cortex (orange arrows), as well as projections crossing the CC that connect with the contralateral prefrontal cortex (blue arrows).

The results of the corticospinal tract analysis [Figure 7] were also consistent with previously reported data. As expected, the descending pathway projected from M1, through the internal capsule, then through the cerebral peduncle, and down to the pyramids of the spinal column. The same pathway could be seen in the results of Holodny et al. (2005) [Figure 8]. We also found a known fiber tract that projects from the corticospinal tract to the cerebellum. Furthermore, our sensitive diffusion tractography also detected minor, known tracts through the motor portion of the thalamus. One projected to the prefrontal cortex and the other passed through the CC to the contralateral prefrontal cortex.

RESOLVING THE LIMITATIONS IN DW-MRI TECHNOLOGY

There are several limitations in using DW-MRI tractography. First, DW-MRI cannot determine the directionality of reconstructed tracts. Additionally, a voxel's diffusion orientation data can be the result of noise, causing in errant tracts that will simply be terminated by a maximum-likelihood approach. PFT, however, is not as affected by noisy data because, instead of terminating, tracts are fully reconstructed and their probabilities calculated. Thus, errant tracts can be distinguished by their low probabilities and subsequently disregarded. Also, the use of longer scanning times reduces noise.

Another limitation of DW-MRI is low resolution, or large voxel size. The typical voxel size is on the order of millimeters whereas axon size is on the order of micrometers. Consequently, many axons travel through a voxel, possibly in many different directions, but only the primary orientation of diffusion is represented by the voxel. One advantage of terminal tracer experiments is that they track projections through single axons by following the diffusion of radioactive markers through those axons.

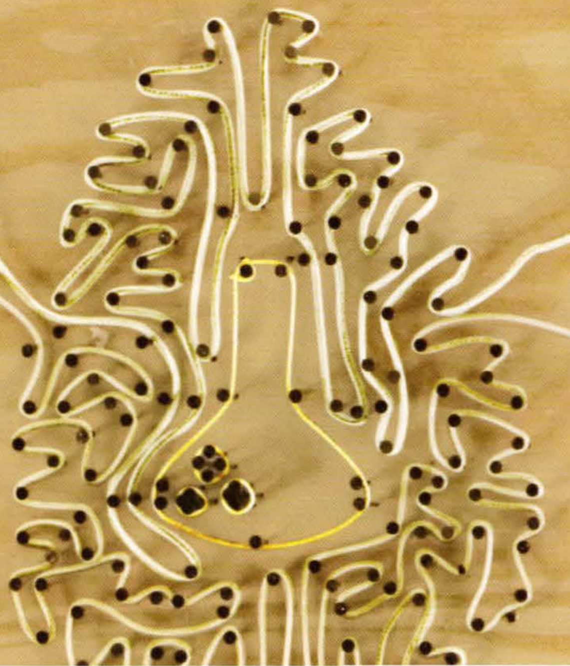

FIGURE 8

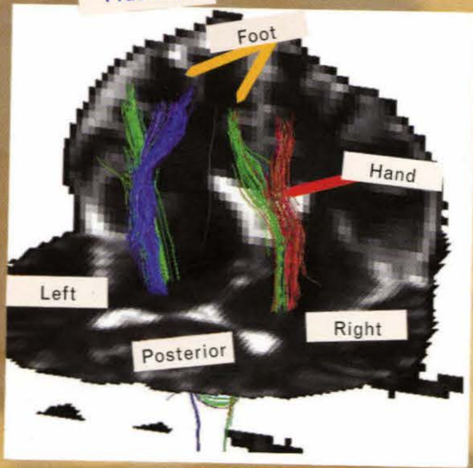

Corticospinal tract reconstructions by Holodny et al. (2005) using diffusion tensor imaging (DTI). The tract passes through the posterior limb of the internal capsule.

However, using MRI with higher field strength, which is not feasible for live subjects, could increase the resolution of DW-MRI. Although current PFT algorithms only incorporate the primary orientation of axons within a voxel, scientists are now attempting to register and employ the minor axon orientations to account for crossing fibers. New algorithms that incorporate minor axis orientations may delineate fiber morphology more faithfully and perform better at tracing fibers through the brain.

APPLICATIONS OF DW-MRI

DW-MRI has great potential for use in clinical and research applications. It offers clinicians the unique ability to measure connectivity *in vivo* so they can quantify developmental and acquired disorders in brain connectivity and assess brain mat-uration in infants and regeneration in healing patients. For researchers, it offers the opportunity to conduct a wide range of connectivity comparisons across different species. Also, connectivity-based clusters can define regional boundaries in the cortex. A further advantage of this technique is that it can be performed on living subjects in conjunction with functional imaging studies on the same individual.Thus, the fiber connections between activated loci can be examined. One interesting application of DW-MRI has been to discern differences in connectivity between musicians and non-musicians as well as between people with varying reading abilities.

The research presented here is noteworthy for its application of DW-MRI. In terms of methodology, it is the first DW-MRI study to use preserved tissue in high magnetic field strength. This allowed for increased image resolution and increased signal to noise ratio. In addition, it is the earliest DW-MRI study to refine segmentation using histology. Our study is also significant because it is the first connectivity analysis of *Gorilla gorilla*. The results of our CC and corticospinal tract studies are similar to past investigations in humans and help to validate the findings. Our accurate results enable us to proceed with additional connectivity measurements. This project is the first step in a larger inter-specific comparison involving the other ape species as well as humans. These comparisons of specific brain connectivity in our closest relatives may provide important information about the evolution of the human brain. □

ACKNOWLEDGMENTS

A Moore Discovery Grant from the California Institute of Technology Brain Imaging Center provided the funding for this research. I acknowledge my mentor, John M. Allman (California Institute of Technology), and my co-mentor, Jason A. Kaufman (California Institute of Technology), for their guidance and technical support. Virginie Goubert performed the histological staining. I am grateful to the Jet Propulsion Laboratory Undergraduate Scholars (JPLUS) program for funding my research fellowship. Finally, I acknowledge the California Institute of Technology and the Summer Undergraduate Research Fellowships (SURF) program for providing this research opportunity.

FURTHER READING

1. *Rye, D.B. Tracking neural pathways with MRI. Trends Neurosci. 22, 373-374 (1999).*
2. *Ramnani, N., Behrens, T.E.J., Penny, W., & Matthews, P.M. New approaches for exploring anatomical and functional connectivity in the human brain. Biol Psychiatry. 56, 613-619 (2004).*
3. *Beaulieu, C., Plewes, C., Paulson, L.A., Roy, D., Snook, L., Concha, L., & Phillips, L. Imaging brain connectivity in children with diverse reading ability. NeuroImage. 25, 1266– 1271 (2005).*

Matthew D. Lew
Xiquan Cui
Changhuei Yang
Department of Electrical Engineering
California Institute of Technology

"Sight is perhaps the most important of our five senses, allowing us to examine the universe around us from up close and afar. However, our eyesight fails us more often than we realize."

Measuring the Phase of Light

SIGHT IS PERHAPS THE MOST IMPORTANT of our five senses, allowing us to examine the universe around us fromup close and afar. However, our eyesight fails us more often than we realize. Take for instance a bird that repeatedly plummets against a spotless window or a biologist who must stain a cell in order to examine its internal features with a microscope. Our eyes are useless when we wish to inspect the structure within transparent objects. Eyes, as well as cameras, ignore a critical characteristic of light – its phase.

Dr. Changhuei Yang and the students in his Biophotonics Laboratory at the California Institute of Technology work to conquer diagnostic and measurement problems in biomedicine. Many of the techniques they use involve characterizing and manipulating the phase of light.

THE NATURE OF LIGHT

Light can generally be described by three parameters: wavelength, amplitude, and phase. The human eye can discern the wavelength, or color, and amplitude, or brightness, of light with ease, but the picture painted by our eyes is incomplete. Our eyes cannot perceive the phase of light. Light is wavelike and periodic in nature; its amplitude varies like a sinusoid as it travels through space. The phase of light describes where the light is as it traces out this sinusoid. Our eyes average or blur this variation over time to allow us to see light's intensity, effectively throwing away the phase information. However there are situations in which a lot of information is encoded within the phase of light.

Microscopy is a particularly good example of an instance where phase is important. Figure 1 shows that differential interference contrast (DIC) microscopy can reveal features that are invisible in normal bright-field microscopy. DIC microscopy reveals variations in the gradient of, or change in, effective optical path length within a sample by using interference, hence the term differential interference contrast. The effective optical path length is proportional to the phase of light and is affected by the sample's index of refraction. Air has an index of refraction equal to 1, while glass has an index of refraction of 1.5. For light waves, traveling through one meter of glass is the same as traveling through 1.5 meters of air; they each have the same effective optical path length. Since the index of refrac-

tion is a material property, many interesting features can be revealed by DIC microscopy.

However, traditional Nomarski DIC microscopy has major disadvantages: its differential phasecontrast images are qualitative, non-linear, and contain both amplitude and phase information. Quantitative phase contrast images are particularly useful in cell biology, with applications ranging from cell dynamics studies to disease pathology. In addition, traditional DIC cannot reliably image anisotropic samples, in which the index of refraction can depend on the polarization axis of the light. This is a major drawback in biological applications, since many organic samples are birefringent. Finally, traditional DIC requires expensive and fragile optical components, including several Wollaston prisms, quarter wave plates, and polarizers.

A NOVEL APPROACH

Our device utilizes the phenomena of interference and diffraction. Interference occurs when two or more beams of coherent light interact with one another; the waves sum together and can interfere constructively or destructively, producing bright and dark fringes. Coherent light refers to light whose rapid fluctuations in amplitude and phase are correlated; light emitted from a laser is an example of coherent light.

Diffraction refers to the bending or spreading of light as it propagates through space. This effect is most pronounced after light passes through an aperture whose size is comparable to its wavelength. The simplest example is the diffraction pattern from a small pinhole. Instead of a stream of particles emerging from the pinhole, light is more accurately pictured as a hemispherical pattern of wavefronts emanating from the pinhole.

We propose an innovative method for performing DIC microscopy that eliminates the aforementioned shortcomings of traditional DIC while being simple and easily integrable for on-chip microscopy. Our device utilizes a commercially available Micron complimentary metal oxide semiconductor (CMOS) grayscale image sensor. This sensor features pixels which are 10 µm x 10 µm in size and can serve as a foundation for microfabrication. We spin-coat a 120 µm thick layer of SU-8, a photoresist which is transparent to visible light, on top of the CMOS sensor. Then, a 20 µm thick layer of aluminum is evaporated on top of the SU-8. Finally, a focused ion beam (FIB) is used to etch two circular holes 500 nm in diameter, with 1 µm center-to-center spacing, in the aluminum. We use a monochromatic light source, a He-Ne laser, to illuminate a sample whose transmitted light propagates through the two holes. The light from the two holes interferes with one another and illuminate our CMOS imager. If there is no phase difference between the light that propagates through the two holes, the resulting interference fringes will be centered directly beneath the holes. However, if there is a phase difference, the interference pattern will translate accordingly. In effect, this device compares the phase of the light propagating through one hole to the phase of the light propagating through the other. By finding the relationship between fringe location and phase differential, we can obtain differential phase information directly from the CMOS camera images.

There are several techniques for building phase images from our differential phase portraits. The most obvious is line integration; each differential phase image can simply be integrated along the phase differentiating direction, or the axis connecting the holes. However, the resulting images will suffer from banding artifacts since the integration constant, which is generally different for each line integral, is thrown away during the differentiating operation performed by the holes. In addition, small phase errors associated with each pixel will accumulate as the line integration proceeds, thereby progressively degrading the image quality.

Another technique becomes apparent when we rewrite $\Delta\phi(x,y)$, the differential phase at location (x,y), as a convolution of two functions using the sifting property of Dirac delta functions:

$$\begin{aligned}\Delta\phi(x,y) &= \phi(x-\tfrac{1}{2}\Delta x, y-\tfrac{1}{2}\Delta y)-\phi(x+\tfrac{1}{2}\Delta x, y+\tfrac{1}{2}\Delta y)\\ &= g(x,y)\otimes\phi(x,y)\end{aligned} \tag{1}$$

where

$$g(x,y)=\delta(x-\tfrac{1}{2}\Delta x, y-\tfrac{1}{2}\Delta y)-\delta(x+\tfrac{1}{2}\Delta x, y+\tfrac{1}{2}\Delta y) \tag{2}$$

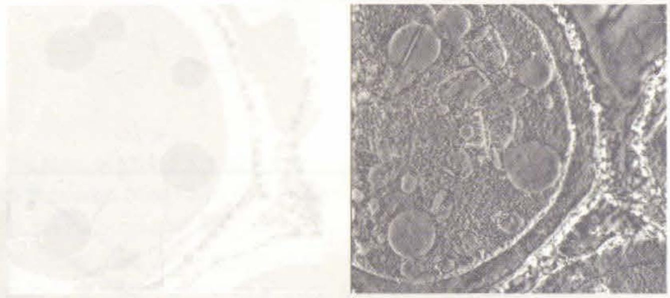

a. b.

FIGURE 1

a. Bright-field image of an unstained liverwort spore,
b. DIC picture of the same spore

These images reproduced from P. J. McMahon, E. D. Barone-Nugent, B. E. Allman, K. A. Nugent: "Quantitative phase-amplitude microscopy II: differential interference contrast imaging for biological TEM"

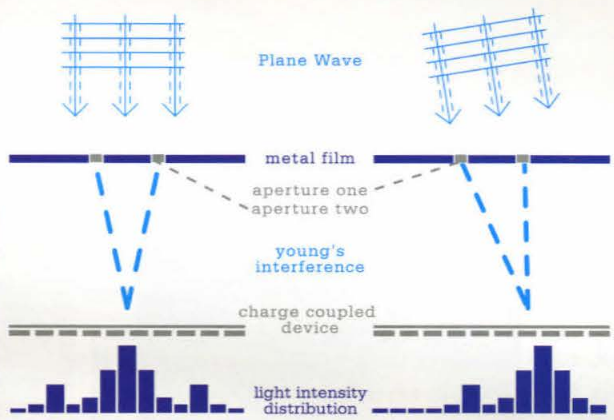

FIGURE 2
Geometry and overall operating principle of our device

$\phi(x,y)$ is the phase at location (x,y), Δx is the separation between the holes in the x-direction, and Δy is the separation between the holes in the y-direction. We can then isolate the phase by performing a deconvolution on (1) and dividing by $g(x,y)$. This process, however, is extremely noise-sensitive and requires the use of a Weiner filter in order to compensate. The optimal choice of filter parameters is subjective and requires the knowledge of the spectral distribution of the signal-to-noise ratio. As a result, reliably constructing quantitative phase information is difficult. A third method involves using the two-dimensional Hilbert transform. This method's primary weakness, however, is that it is not quantitatively accurate and therefore not useful for our application.

SIMULATIONS OF OUR DEVICE

Rigorously simulating the phase responsivity of this device requires us to numerically solve Maxwell's equations for our three-dimensional geometry, a task which is extraordinarily computationally expensive. However, by utilizing the Fraunhofer (far-field) approximation, we can greatly simplify the diffraction simulations. Consider the case where monochromatic light is incident upon an aperture, where

$$p(x,y) = \begin{cases} \exp(i\phi), & \textit{inside the aperture} \\ 0, & \textit{outside the aperture} \end{cases} \quad (3)$$

is the aperture function and ϕ represents the phase of the light propagating through the aperture. The diffraction pattern seen on

$$I(x,y) = \frac{I_i}{(\lambda d)^2}\left|P\left(\frac{x}{\lambda d},\frac{y}{\lambda d}\right)\right|^2 \quad (4)$$

a viewing screen is just the Fourier transform of the aperture function where I_i is the intensity of the incident light, λ is the

$$P(\upsilon_x,\upsilon_y) = \int_{-\infty}^{\infty}\int_{-\infty}^{\infty} p(x,y)\exp\left[i2\pi(\upsilon_x x+\upsilon_y y)\right]\,dx\,dy \quad (5)$$

wavelength of the incident light, and d is the distance between the aperture and the viewing screen. The validity of this approximation is assured by the "antenna designer's formula," which states that

$$d > \frac{2D^2}{\lambda} \quad (6)$$

where D is the linear dimension of the aperture. For our device, d is 1.5 µm and λ is 632.8 nm for our He-Ne laser, which implies that must be greater than 7.11 µm in order for the Fraunhofer approximation to hold. Since our CMOS imager is 120 µm below our holes, we satisfy this condition with two orders of magnitude to spare.

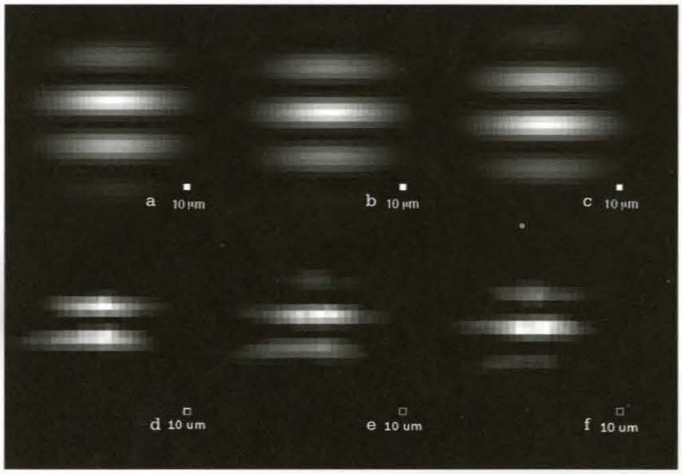

FIGURE 4

a) Simulated fringes produced by a -90° phase differential, b) simulated fringes produced by a 0° phase differential, c) simulated fringes produced by a 90° phase differential, d) measured fringes produced by a -90° phase differential as imaged with our device, e) fringes produced by a 0° phase differential, f) fringes produced by a 90° phase differential; device parameters are an illumination wavelength of 632.8 nm, two 500 nm diameter holes with 1 µm center-to-center spacing, 120 µm distance between holes and CCD pixels, and 10 µm x 10 µm CCD pixels

Using MATLAB, we modeled our aperture as a two-dimensional matrix and performed a fast Fourier transform (FFT) on it to find the diffraction pattern. We found that the diffraction pattern comprises three interference fringes. Furthermore, the simulations proved that these fringes shift as a function of the phase differential. This analysis was achieved quantitatively by using the curve-fitting tool within MATLAB to fit the zero-order, or center, fringe to a Gaussian curve, yielding a center location for that fringe. Mapping the fringe locations to their corresponding phase differentials produced a linear relationship across a 180 degree range of phase differentials.

Further simulation showed that larger holes create brighter fringes, and holes that are closer together produce larger fringes. These trends suggest that we should use the largest holes with the closest spacing, but there are fundamental physical limits. First, larger holes lower our spatial resolution, since we are comparing the phase between two circular sources of light instead of two point sources of light. Second, the two holes will couple light between one another when their spacing goes below a certain distance; instead of two small holes, we effectively have one large hole. This occurs because there is not enough metal between the two holes to attenuate the electromagnetic waves traveling between the two holes.

INITIAL IMAGES

Upon fabrication completion, our first task was to measure the phase responsivity of our device. We directed a collimated He-Ne laser beam onto our holes and mounted our device on a rotating stage, ensuring that the rotation direction of the stage was parallel to the axis connecting the two holes. Since the center-to-center spacing of the holes was much smaller than the laser beam width (1 µm versus 1 mm), we approximated the incident beam as a plane wave. If the laser beam is normal to our holes, there is no path length difference, and therefore no phase difference, between the light propagating through the two holes. We therefore controlled the phase difference between the two holes by rotating our device. A responsivity curve was created by mapping how phase differential corresponds to fringe location. The slope of the measured responsivity curve deviates from the theoretical curve by 25 percent. This is most likely due to the assumptions made in our simulations. By employing the Fraunhofer approximation, we implicitly assumed that scalar diffraction theory applies to our device. However, our aperture size is on the order of the light's wavelength. As such, the interaction of light at the dielectric interface between aluminum and air is significant. These coupling effects are ignored in our scalar diffraction model. Thus, accurate, quantitative simulations require numerically solving Maxwell's equations for our geometry.

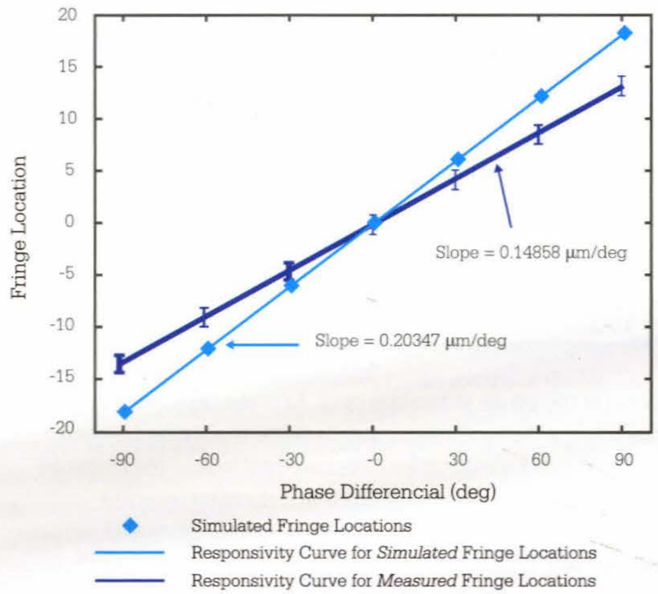

FIGURE 5
Simulated versus measured responsivity curves. Error bars represent the variation in measured fringe location at each phase differential.

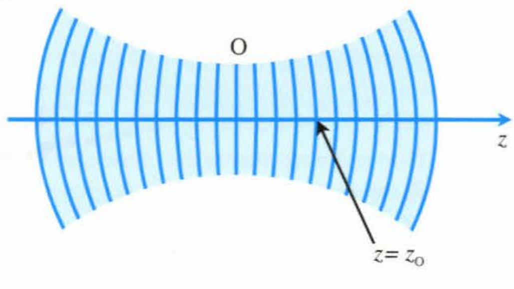

FIGURE 6
Wavefronts and regions of a Gaussian beam. The wavefronts are approximately planar near the waist and spherical far from the waist.

We then scanned a well-known phase profile to test our device. A Gaussian beam was chosen for its familiar behavior and because it can be generated and modified easily. Laser beams are Gaussian in nature, and Gaussian beams propagating through circularly symmetric optical components, such as lenses, remain Gaussian. The intensity of a Gaussian beam propagating in the z-direction is given by

$$I(x,y,z)=\frac{2P}{\pi W^2(z)}\exp\left[-\frac{2(x^2+y^2)}{W^2(z)}\right] \tag{7}$$

where

$$W(z)=W_0\left[1+\left(\frac{z}{z_0}\right)^2\right]^{\frac{1}{2}} \tag{8}$$

P is the beam's power, W_o is its minimum waist size, and Z_o is the Rayleigh range of the beam. $W(z)$ characterizes the expansion of the beam's cross-section as the beam propagates, and larger Rayleigh range values lead to slower beam expansion. As (7) shows, Gaussian beams are radially symmetric in the transverse or xy plane. Gaussian beams have three regions of interest for phase profiling: a converging section, the waist, and a diverging section [Figure 6]. The beam's phase profile is steepest far away from the beam waist and becomes progressively flatter towards the beam waist. We expect the phase portraits of the Gaussian beam to be bell-shaped, oriented upwards or downwards depending upon whether the beam is converging or diverging. The differential phase profiles should exhibit a zero degree phase differential near the center of the beam and be monotonic in the differentiating direction.

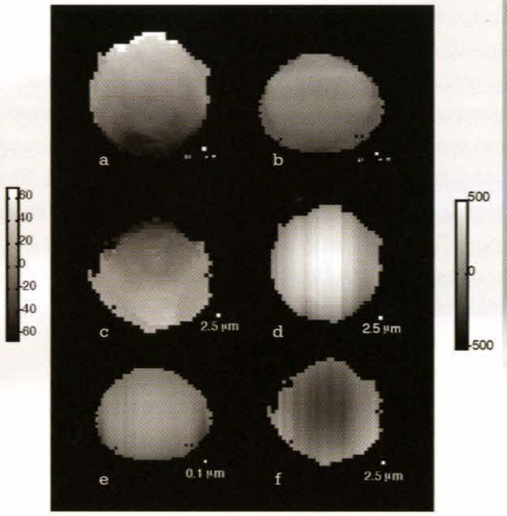

FIGURE 7

a) Differential phase profile of a converging Gaussian beam, b) differential phase profile of a beam's waist, c) differential phase profile of a diverging beam, d) reconstructed phase profile of a converging Gaussian beam, e) phase profile of a beam's waist, f) phase profile of a diverging beam; all color bars are in units of degrees

We imaged a Gaussian beam at each of its three sections to show the different phase and differential phase behavior associated with each section. The line integration method was used to construct phase profiles from the differential phase images, and vertical banding results since the axis connecting the holes, and thus the integrating direction, is vertical. Note the contrasting differential phase profiles between converging and diverging Gaussian beams, as well as the relatively flat profile of the beam's waist. In addition, the circularly symmetric phase profiles of the Gaussian beams are worth noting.

FUTURE DIRECTIONS

The major disadvantage of our current device is that it only differentiates phase in a single direction, making a full reconstruction of a sample's phase profile impossible. We have numerically simulated the behavior of a couple of geometries that would enable us to gather two-dimensional differential phase data. We plan to test these geometries in the lab in the near future.

We also plan to begin applying the technique and evaluating its performance for different applications. Besides the obvious biological applications, our technique is well suited for singular optics studies. Singular optics studies optical phenomena which contain one or more phase singularities, or areas where phase is undefined. These wavefronts have unusual phase behavior, and our device is well-suited to study them.

Optical vortices are prevalent in the world of singular optics. They can be described by the envelope function

$$u(\rho,\phi,z) = A_m(\rho,z)\exp(-im\phi)\exp\left[i\varphi_m(\rho,z)\right]$$

in cylindrical coordinates where the phase components are separable into a portion dependent on ϕ and a portion dependent upon p and z. m is the topological charge and is always an integer to satisfy phase continuity. The $exp(-im\phi)$ term is the most important, giving the optical vortex its characteristic helical wavefront. In any cross-section of an optical vortex where z is constant, phase is proportional to polar angle.

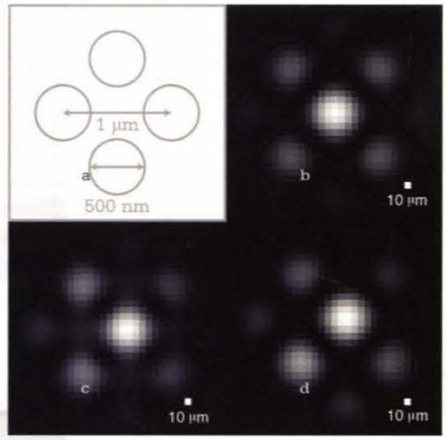

FIGURE 8
a) geometry for imaging 2D differential phase using 4 holes, b) simulated fringes from the 4 hole device with a 0° phase differential in both directions, c) fringes from the 4 hole device with a 90° phase differential in the horizontal direction, d) fringes from the 4 hole device with a 90° phase differential in both directions; simulation parameters are an illumination wavelength of 632.8 nm, 120 μm distance between holes and CCD pixels, and 10 μm x 10 μm CCD pixels

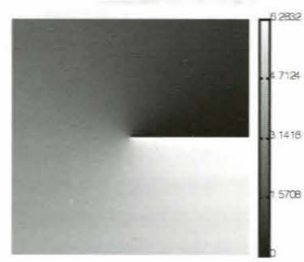

FIGURE 9
Phase profile of an optical vortex with a topological charge of 1.There is a phase singularity, and a corresponding point with zero intensity, at the center of the vortex.

There are many methods for generating optical vortices including spiral phase plates, fractal zone plates, or interfering three plane waves. However, the most practical methods utilize spatial light modulators (SLMs), computer-generated holograms (CGHs), or a combination of the two. We have computed the CGHs required to generate optical vortices of various topological charges. An advantage of employing our device to profile optical vortices is its ease of use. Conventional techniques for verifying the existence of optical vortices require interfering them with a plane wave and observing the resulting interference pattern. Our device would eliminate this tedious process and allow the quality of the optical vortex to be examined directly. We plan to perform differential phase imaging of these structures in the near future.

Although there is a significant error associated with utilizing scalar diffraction theory to predict the phase sensitivity of our device, we found that our device provides quantitative DIC images with high spatial resolution and phase sensitivity. Differential phase images of a Gaussian beam were captured with our device, enabling the partial construction of the beam's phase profile. Our technique has the advantages of being compact, low cost, and easily adaptable for on-chip microscopy. Furthermore, we can study diverse samples using our device, such as biological structures and optical vortices. □

ACKNOWLEDGEMENTS

I thank Professor Changhuei Yang and Xiquan Cui for their mentorship throughout this Summer Undergraduate Research Fellowship. I also appreciate the timely advice of Xin Heng, Jigang Wu, and Zahid Yaqoob as I endured the trials and tribulations that are the research process. I extend my gratitude to Mr. and Mrs. Anthony Skjellum for funding a considerable portion of my project. It is the donations of generous alumni like these that keep the Summer Undergraduate Research Fellowship alive at Caltech.

FURTHER READING

1. E. D. Barone-Nugent, A. Barty, and K. A. Nugent, "Quantitative phase-amplitude microscopy I: optical microscopy," Journal of Microscopy-Oxford 206, 194-203 (2002).

2. P. J. McMahon, E. D. Barone-Nugent, B. E. Allman et al., "Quantitative phase-amplitude microscopy II: differential interference contrast imaging for biological TEM," Journal of Microscopy-Oxford 206, 204-208 (2002).

3. M. R. Arnison, K. G. Larkin, C. J. R. Sheppard et al., "Linear phase imaging using differential interference contrast microscopy," Journal of Microscopy-Oxford 214, 7-12 (2004).

4. Bahaa E. A. Saleh and Malvin Carl Teich, Fundamentals of Photonics. (John Wiley & Sons, Inc., New York, 1991).

5. Joseph W. Goodman, Introduction to Fourier Optics, 3rd ed. (Roberts & Company Publishers, Englewood, 2005).

6. Z. S. Sacks, D. Rozas, and G. A. Swartzlander, "Holographic formation of optical-vortex filaments," Journal of the Optical Society of America B-Optical Physics 15 (8), 2226-2234 (1998).

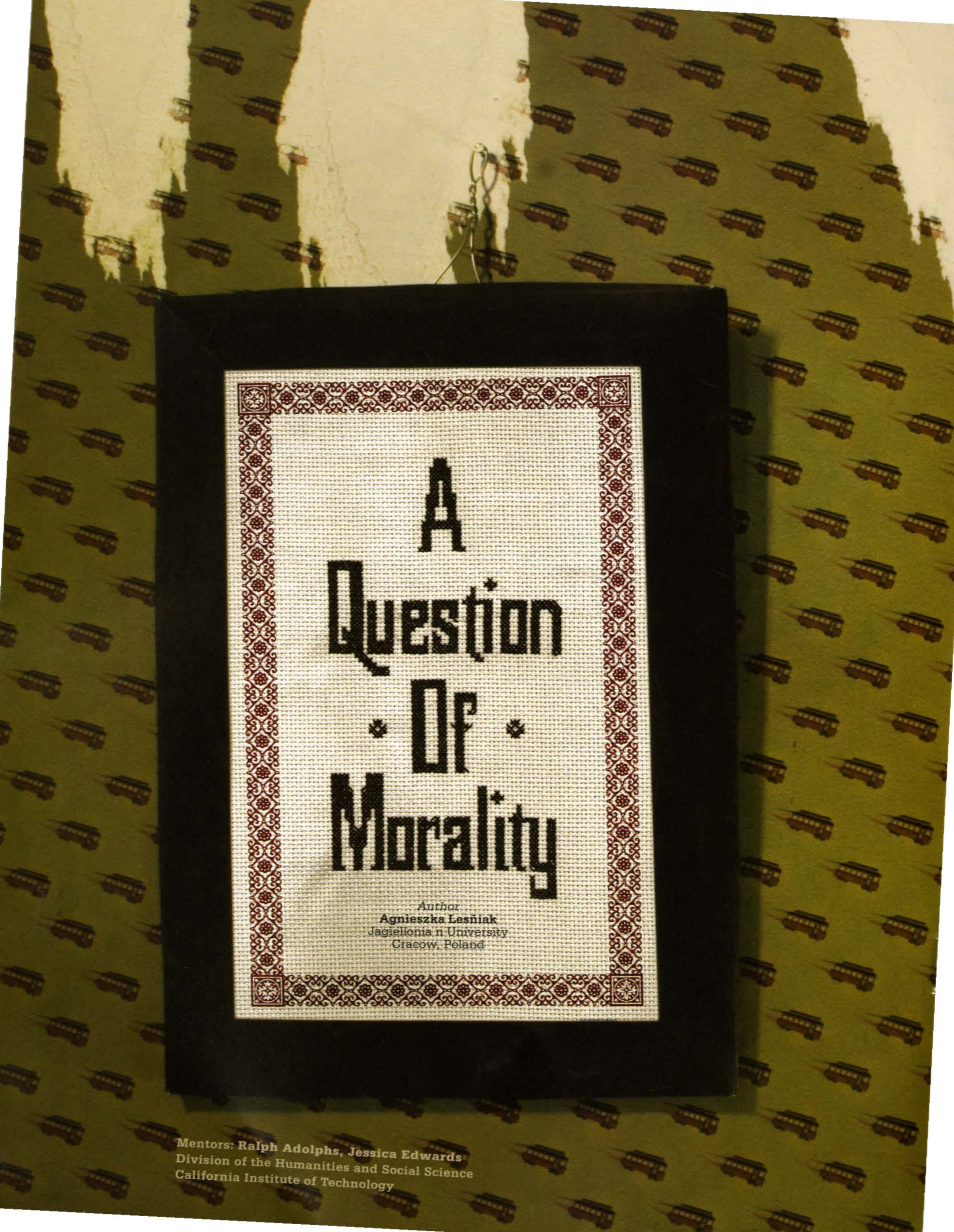

Mentors: **Ralph Adolphs, Jessica Edwards**
Division of the Humanities and Social Science
California Institute of Technology

SUPPOSE THAT A RUNAWAY TROLLEY IS HEADED towards a group of five people who will certainly be killed if it proceeds on its current course. You watch in horror as the trolley rushes toward the utterly oblivious group when suddenly, in a flash of inspiration, you realize that with a flip of a switch, the trolley can be diverted towards another set of tracks to save the group. Glancing at the second track, you see with anguished indecision that another person will be killed if the switch is flipped. What do you do?

Now, suppose the same trolley is headed towards the same group of five people, but this time, you notice that a very large person is standing near the tracks. Rapidly assessing the situation with mental calculations, you realize that if you push him into the trolley's path, the trolley's resulting velocity will be sufficiently slow to save the five people at the expense of his life. What do you do now?

"Rapidly assessing the situation with mental calculations, you realize that if you push him into the trolley's path, the trolley's resulting velocity will be sufficiently slow to save the five people at the expense of his life."

If you would flip the switch to save the group of people in the first scenario, you are in the majority. On the other hand, if you said that you would push the large man onto the tracks to save the group in the second scenario, you are in the minority. The details of each dilemma, however, are essentially the same in that one person's life will be sacrificed to save five others. Why, then, do most people consider action in one situation ethically correct and action in the other immoral when the outcome is identical?

The classic questions described above have given moral psychologists the responsibility of explaining the discrepancy in response to the two scenarios. For decades, researchers have investigated what instinctively makes people amenable to one case while repulsed by the other. Several possible solutions have been suggested with the intent of improving scientific insight into human morality and judgment. Current theories explain the difference as arising from the engagement of a key component of moral judgment: emotion.

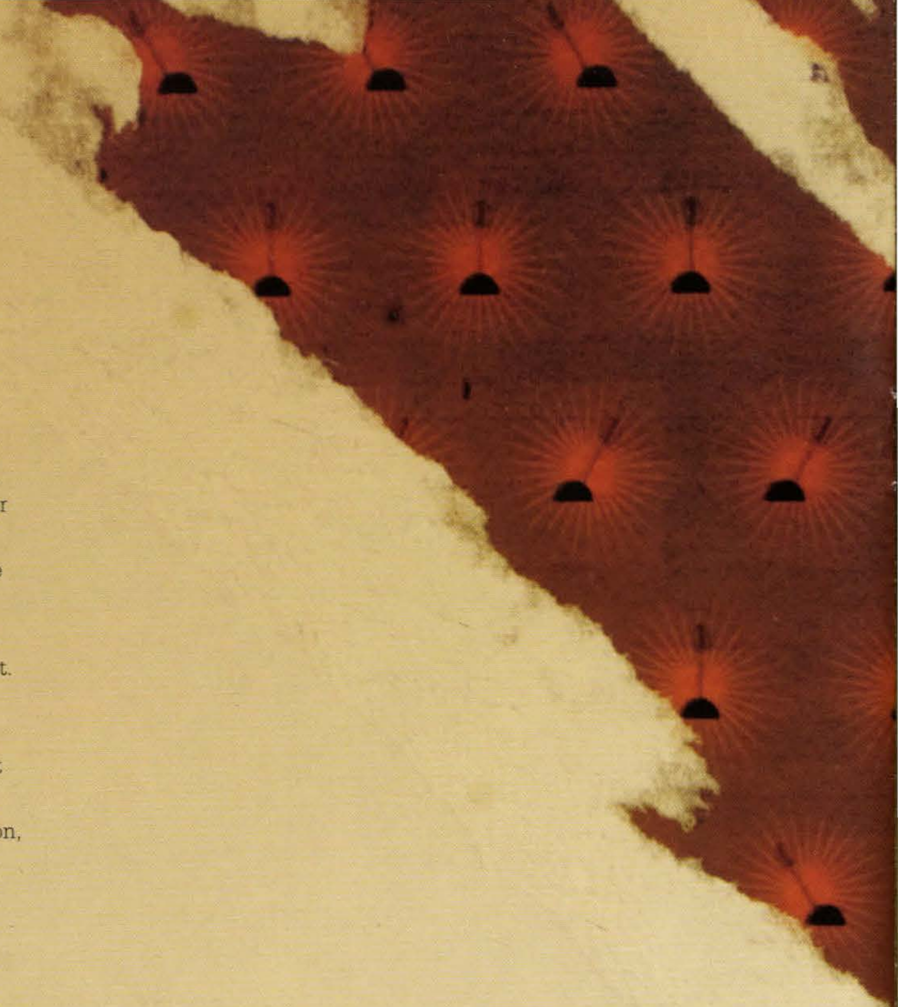

DEVELOPMENT OF MORAL PSYCHOLOGY

Social psychology was not widely regarded as a science until the cognitive revolution of the mid-20th century, during which Lawrence Kohlberg developed a six-stage model of the development of moral reasoning. According to Kohlberg, moral growth is driven not by simple brain maturation but rather by experience in "role-taking," or looking at a problem from multiple perspectives in order to develop a more comprehensive view. Kohlberg claimed that by expanding the breadth of experience, role-taking improved moral reasoning. Subsequently, the improved moral reasoning could drive better moral judgment.

However, Kohlberg's focus on moral reasoning seems to ignore the importance of moral emotions. Moral emotions are defined as the set of emotions that affect an individual's interest in the welfare of others. In community environments, this can be manifested in social phenomena such as altruism, cooperation, and conformity. Some specific examples of moral emotions are sympathy, gratitude, and vengeance.

The social intuitionist model, a recent comprehensive model that attempts to resolve the oversights in Kohlberg's theories, suggests that moral judgment is much like aesthetic judgment: a person sees an action or hears a story, and he has an instant feeling of approval or disapproval. While Kohlberg asserted that moral judgments are inspired by reason, this model argues that most moral judgments stem from intuition and instinct. Social intuitionists believe that people certainly do engage in moral reasoning, but these processes are typically one-sided efforts to support their intuitive conclusions.

EVIDENCE OF EMOTIONS IN ETHICS

In 2001, Greene et al. performed an experiment to study the activity in specific areas of the brain while the subject considered various moral dilemmas. The two trolley problems previously described were the scenarios used and are easily categorized as personal and impersonal moral judgments. Greene et al. defined impersonal violations as actions that caused bodily harm to another person as a foreseen side-effect, but not a direct intention. A moral violation is personal if it directly and intentionally causes harm to another person as a means to achieve the desired outcome. In the case with the switch, one does not intend harm towards anyone; harming another is simply an unavoidable side-effect of rescuing the group of five. Consequently, the switch case can be classified as an impersonal violation. However, in the case with the large man, harming the man is an integral part of the plan to save the group. Direct participation in the inflicted harm that is inherent in the moral action makes this a personal violation.

Greene et al. presented the trolley problems to subjects and, while they deliberated about what the morally right choice was, measured their brain activity with functional magnetic resonance imaging (fMRI). fMRI, one of the most recent developments in neural imaging, is the use of magnetic resonance imaging to measure the hemodynamic response, or changes in blood flow, related to neural activity of the subject. Greene et al. found activity in brain regions associated with reason and emotion.

The study showed that the deliberation resulting in personal and impersonal moral judgments can be distinguished by the corresponding patterns of brain activity. Greene et al. established that while considering personal moral dilemmas, subjects demonstrated increased activity inareas associated with social and emotional processing. In contrast, impersonal and non-moral dilemmas showed increased activity in areas associated with working memory, which refers to processes used for the manipulation of information. The study also showed that while subjects were slow to approve of personal violation, their approvals and disapprovals of impersonal moral and non-moral judgments were both quite short. The collective results support the theory that the subject must overcome his immediate negative emotional response before condoning personal moral violations. Such a battle of wills is not necessary with less emotionally-charged actions. Consequently, Greene et al. claim that human moral thinking is not simply one specific process, but rather a complex interplay between two distinct processes: social-emotional responses to the situation and standard reasoning as applied to moral contexts.

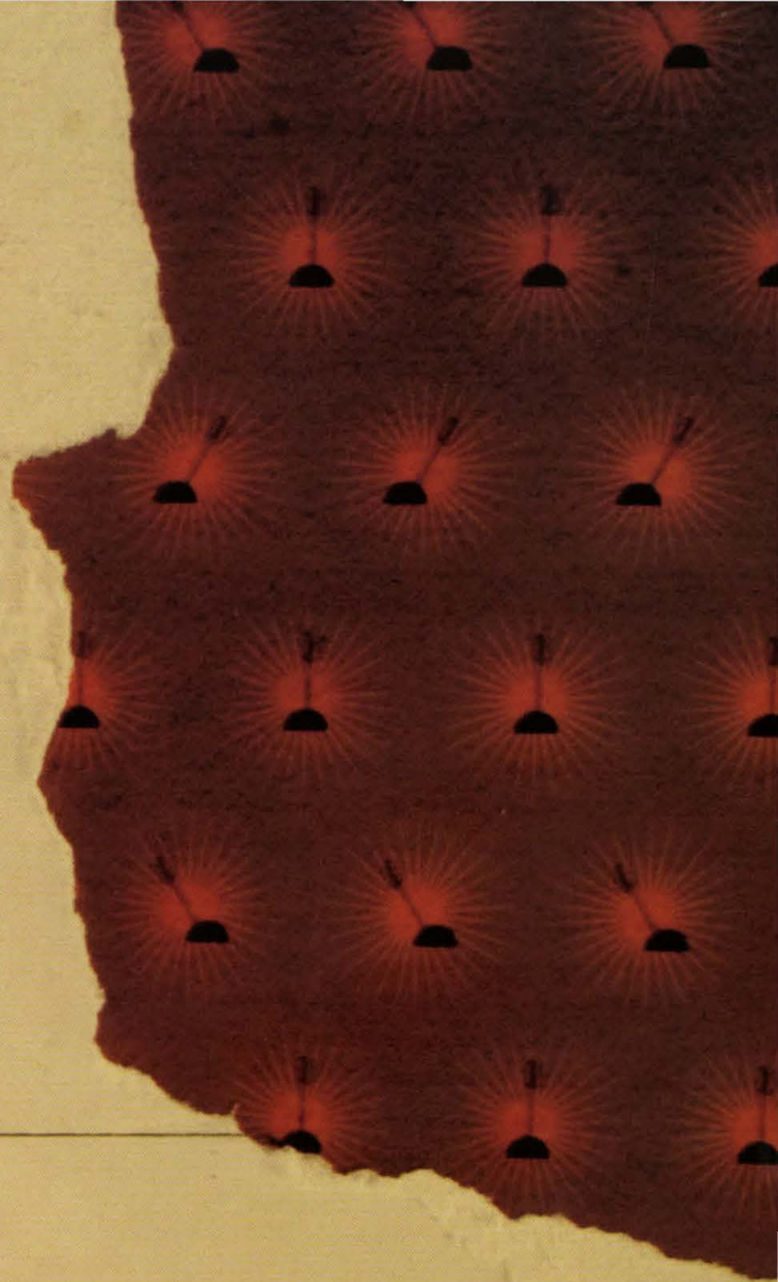

AUTOBIOGRAPHICAL EVENTS INVOLVING MORAL DECISION

Research in the Adolphs laboratory at the California Institute of Technology has recently focused on ethical judgment in autobiographical memories. The dissertation work of Jessica Edwards, a biology graduate student in the lab, investigates how people recollect emotional autobio-graphical events and how they make moral judgments. The present research focuses on elucidating the kinds of moral memories that people remember from their lives, and how these might differ between people. A database of real moral stories was developed over the last two years, forming the data on which the analyses that comprised this study were based.

To construct this database, subjects aged 40 to 60 were recruited online and screened for fluency in English. All had been Southern California residents for at least 15 years. Subjects came into the lab and were shown a series of words about which they had to recollect a memory, e.g. "Tell me about a time you felt guilty." A total of 4000 autobiographical memories were collected and 749 of these were classified as moral stories. To be classified as a moral story, the stories had to be personal and involve a specific episode from the subject's past. Furthermore, they needed to have an element of moral judgment either from the perspective of the narrator or the reader.

In another part of the project, a group of 52 subjects, called raters, were then used to evaluate these moral stories. The raters read subsets of the transcribed moral stories and completed questionnaires about the narrator's background as well as specific emotions associated with the event. The questions covered the nature of the moral decision, justificationfor it, emotional aftermath, and possible cue words that could have elicited the memory. A story involving shoplifting, for example, can be explained by greed and the subject may have regretted his decision afterwards. Cue words in this case could include doubt and remorsefulness.

CATEGORIZATION OF AUTOBIOGRAPHICAL EVENTS

The Variance Maximizing (Varimax) rotation was applied to obtain clear relations between the factors. In this method, we rotated the coordinate axes of a scatter plot until the X-axis approximated the regression line. Because the goal of the rotation is to maximize the variance of the new variable while minimizing all other variance, this type of rotation is called variance maximizing.

Statistical analysis on the moral autobiographical events and the evaluations was used to determine the emotional factors involved in moral judgment. We divided the dataset of 749 moral autobiographical stories into 174 positive stories and

575 negative stories. Each group was analyzed separately.

The aim of this study was to determine non-intuitive categories that might be used to categorize moral concepts. Because the non-intuitive categories are difficult to conceptualize, it would be very instructive to try to identify them based on the ratings data set. We used factor analysis to explain the variance among the 749 moral stories to just a few statistically-relevant factors. Factor analysis, a statistical technique used to explain variability among observed random variables, assumes that the rating data on different attributes can be reduced down to a few important dimensions or qualities.

We found three main categories of common moral events that are often encountered on a daily basis. All calculations were done with the help of the program STATISTICA. We began by conducting hierarchical cluster analysis, a type of data segmentation based on the degree of similarity or dissimilarity between the individual events being clustered. Agglomerative methods were used, meaning that a number of stories were linked together to form growing clusters of increasingly dissimilar elements. When all the stories were joined, the data contained clear clusters of similar objects. In the hierarchal tree diagram, these clusters can be identified as distinct branches [Figure 1].

The complete linkage method was used to determine if two clusters were sufficiently similar for linkage. In this method, the distances between clusters were determined by the greatest distance between two objects in the different clusters, labeled in the study as "furthest neighbors." From cluster analysis, we were able to establish two distinct data groups: a positive stories subset (involving actions such as altruism or cooperation) and a negative stories subset (involving lying or cheating).

Both the positive and negative subsets of stories were then manipulated with the Scree test, a method of factor analysis used to explain variability among observedrandom variables. It assumes that the rating data on different attributes can be reduced down to a few important dimensions or qualities. These dimensions can be determined through an evaluation of the area of a graph of eigenvalues in which the plot appears to level off [Figure 2]. The region to the right of this point can be identified as the "factorial scree," where scree refers to the geological term indicating the collection of debris on the lower part of a slope. The Scree test showed only one factor for the positive stories and three factors for the negative stories.

❖ FIGURE 1 ❖

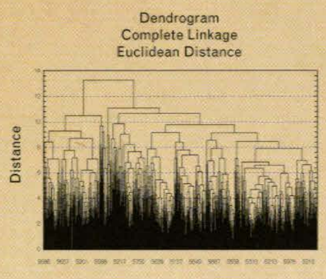

FIGURE 1 Hierarchical Tree Diagram
Autobiographical stories involving moral judgment were analyzed through cluster analysis by linking stories together to form clusters of similar elements. The x-axis is the number assigned to each story. Each cluster can be identified in the hierarchical tree branch diagram as a distinct branch. The positive memories aggregated into one cluster on the left whereas the negative moral memories formed multiple clusters on the right.

❖ FIGURE 2 ❖

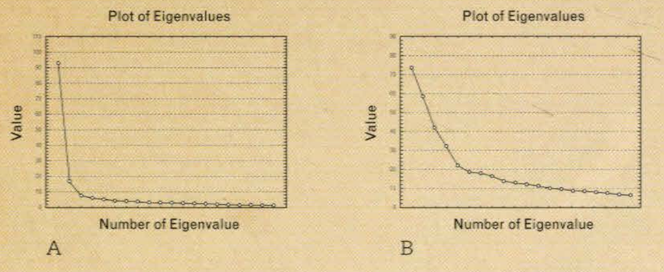

FIGURE 2 Scree Tests
The (a) positive stories subset and (b) negative stories subset were manipulated with the Scree test, which assumes that the rating data on different attributes can be reduced to a few important dimensions or qualities. These dimensions can be determined through an evaluation of the area of a graph of eigenvalues in which the plot appears to level off. The identified factors are indicated by the black arrows.

DETERMINATION OF FACTOR RELATIONSHIPS

Once the collection of 749 moral autobiographical stories was reduced to a total of four factors by the Scree test, further analysis was done on these factors to elucidate any possible correlations among them.

The Variance Maximizing (Varimax) rotation was applied to obtain clear relations between the factors. In this method, we rotated the coordinate axes of a scatter plot until the X-axis approximated the regression line. Because the goal of the rotation is to maximize the variance of the new variable while minimizing all other variance, this type of rotation is called variance maximizing.

The factors in the subset of negative stories have proved to be orthogonal to each other, and consequently, we identified distinct categories with the same origin [Figure 3]. Alternatively, the graph of the factors in the positive stories subset [Figure 4] is homogenous. We concluded that there is only one main factor for this subset of stories.

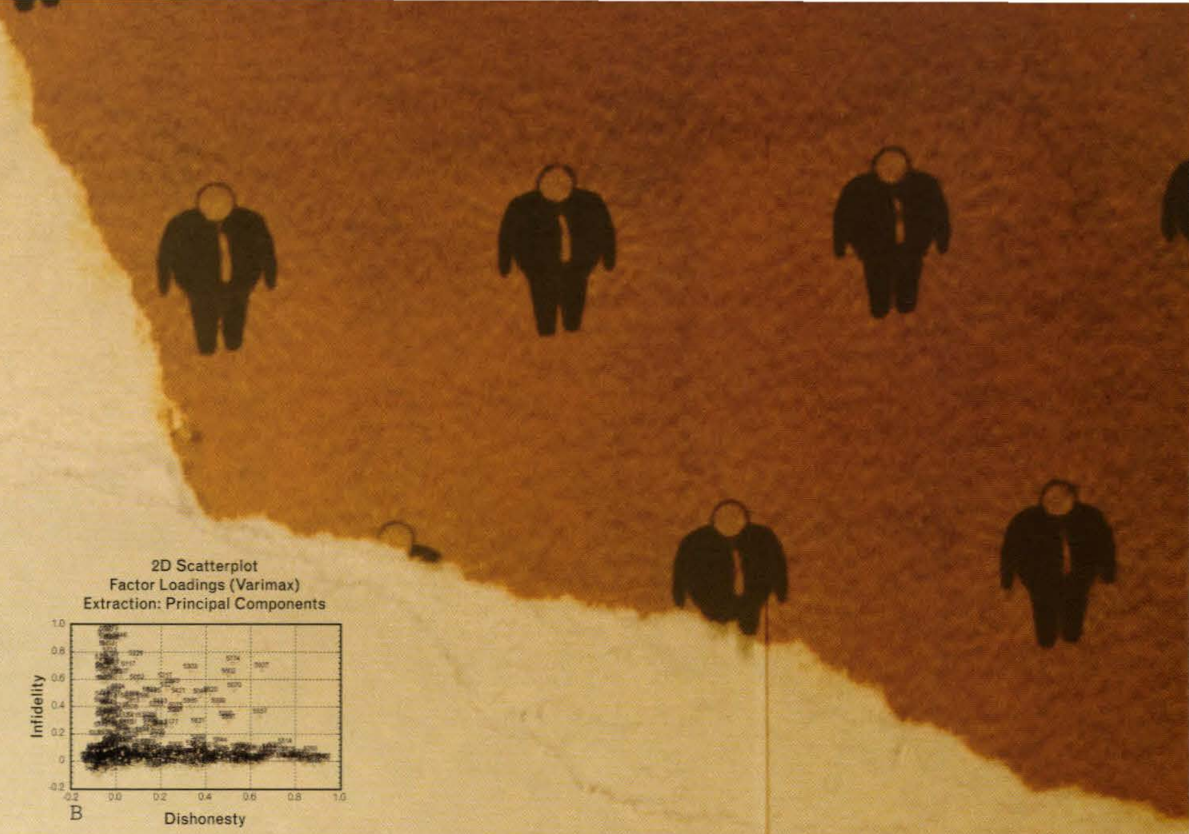

✧ FIGURE 3 ✧

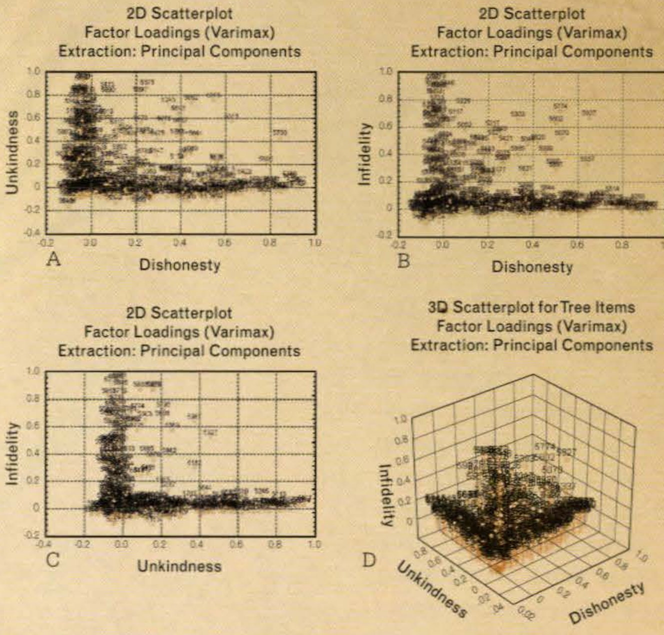

FIGURE 3 Varimax Rotation on Negative Story Subset
The Variance Maximizing (Varimax) rotation was applied to obtain clear relations between the factors. In this method, we rotated the coordinate axes of a scatter plot until the x-axis approximates the regression line. In these cases, the following factors have proved to be orthogonal to each other:
(a) Dishonesty and Unkindness
(b) Unkindness and Infidelity
(c) Dishonesty and Infidelity
(d) Dishonesty, Unkindness, and Infidelity

✧ FIGURE 4 ✧

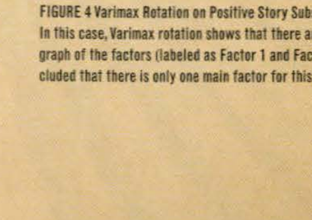

FIGURE 4 Varimax Rotation on Positive Story Subset
In this case, Varimax rotation shows that there are no orthogonal factors. The graph of the factors (labeled as Factor 1 and Factor 2) is homogenous. We concluded that there is only one main factor for this subset of stories: altruism.

FACTORS OF MORAL JUDGMENT

The factors obtained through the analysis were then evaluated in terms of our daily social experiences. We made an attempt to assign a name to each factor and trace it back to its emotional features. In the negative stories subset, we recognized three factors: dishonesty, unkindness, and infidelity. In the positive stories subset, we found altruism to be the only factor.

As a result of the objective methods applied to study the triggers of moral memories, we have found out more about the human psyche, particularly the thought processes involved in making moral judgments. The results of the study may prove useful in studying moral reasoning in social contexts and may broaden our knowledge of human behavior. □

ACKNOWLEDGEMENTS

I would like to express my deepest gratitude to my mentors, Professor Ralph Adolphs and Jessica Edwards, for their invaluable help and guidance throughout the SURF project. I would also like to thank the SURF program and its staff for giving me this opportunity to visit Caltech.

Seeing Magnetic Fields

Jun Young Kim
University of Cambridge

Mentors

Professor Paul M. Bellan
California Institute of Technology

Gunsu Yun
California Institute of Technology

MAGNETIC FIELDS ARE UBIQUITOUSLY USED IN MODERN technology. From biomedical purposes such as magnetic resonance imaging to high-speed Maglev trains utilizing superconductivity, magnets are indispensable to society. The powerful, yet invisible phenomenon of magnetic fields is applied effectively in guiding charged particles. The utility of the magnetic field would be enhanced if we could 'see' it. Instead of following a compass, wouldn't it be great to just to follow a visible line? Unfortunately, while the technology for generating magnetic fields is highly evolved, the methods for visualizing them are still primordial. In closed systems, such as inside a large vacuum chamber, a more convenient mechanism for imaging the magnetic fields needs to be devised. On the way towards developing better technology for viewing magnetic fields, an apparatus was constructed that can illuminate the lines of magnetic fields with electron beams in a low pressure system.

FOLLOWING THE PATH

The path of an electron can be observed in the following way. An electron traveling through a magnetic field is accelerated in the direction that is determined by the cross product between its velocity and the field direction, or v x B. The resultant motion is a helical motion parallel (and anti-parallel) to the direction of B field [Figure 1]. The radius of this helical motion is called the Larmor radius, and it is determined by $r = m v / e B$. Therefore, with a low velocity electron and a strong magnetic field, the Larmor radius diminishes to the order of millimeters or less.

In a standard experiment to measure the electron charge to mass ratio, one can visualize the electron path in a low pressure gas system composed typically of argon or mercury. While the electron beam orbits with a known magnetic field, the Larmor radius is measured visually. The same theoretical concept is employed in this study, but the radius is made small so that the trajectory is seen to be continuous, aligning the lines of the magnetic fields.

TO BE SEEN

When an electron travels through a low pressure helium gas it collides with gas atoms. In this collision, the electron transfers a part of its kinetic energy to the helium atom. The helium atom then gets 'excited' and some molecules of gas will subsequently emit visible radiations in order to return to a lower energy state.

Since the two aforementioned processes happen simultaneously, electrons move in helical trajectories while being illuminated by helium light-excitations. Since it has a small Larmor radius, the electron beam will be aligned to the directions of the background magnetic fields. In static and dynamic systems, this feature can be exploited to visualize the magnetic field through capturing the images of the beam illumination in static and dynamic systems.

The experiment was carried in four steps: (i) create a low pressure helium system, (ii) produce thermionic electrons, (iii) accelerate electrons to form a beam, and (iv) apply magnetic fields while observing the beam.

"In static and dynamic systems, this feature can be exploited to visualize the magnetic field through capturing the images of the beam illumination in static and dynamic systems."

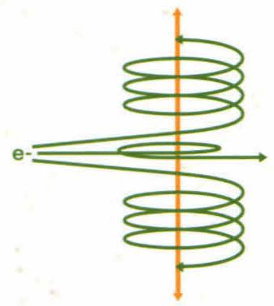

FIGURE 1

Parallel, stationary, and anti-parallel motions of electrons near a magnetic field line. The Larmor radius of these motions depends on the electron velocity and magnetic field strength.

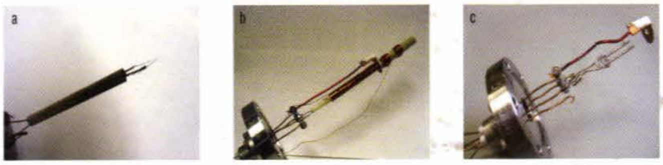

FIGURE 2

Changes in electron gun designs. a) A 0.004 inch diameter tungsten wire at the tip is spark-welded to electrodes.The ceramic tube prevents unwanted contacts between electrodes. b) A metal plate in front of the filament now accelerates electrons from the filament.This frees the region outside the plate from electric field c) Tungsten filaments were replaced by iridium filament to improve the filament durability.The filament was later covered with kapton sheet and aluminium foil.

BUILT THIS WAY

A stainless steel vacuum chamber with the internal volume of about 500 ml was used to create a low pressure He system. First, the chamber was emptied with a TribodyneTM pump to a moderate vacuum pressure of 10-3 Torr. The chamber was then filled with helium gas until the internal pressure reached about 50 mTorr using a gas leak valve. The optimal gas pressure was calculated using the ideal gas equation of state, and the collision cross-section was assumed to be of a neutral gas, 3×10^{-20} m^2. At pressures between 50 to 500 mTorr, the mean free paths of helium atoms vary between 0.2 to 2 cm. These lengths were chosen so that the electron beam does not scatter off too easily.

In order to produce electron beams, an electron gun unit was assembled and attached to the chamber [Figure 2]. Thin tungsten wires of diameters 0.004 inch, 0.005 inch and 0.0065 inch were used together as a filament that produced electrons thermionically when heated. Thermionic emission is also called the Edison effect. Using the Richardson-Dushmann equation, it is possible to estimate the amount of thermionic electrons that are emitted at a given temperature. The filament needs to be at 2000 K or above to produce a detectable amount of thermionic electrons. Tungsten was chosen since it has the highest melting point amongst metals. Assuming the tungsten radiates as a blackbody, the temperature could roughly be guessed from its color when glowing.

The electrons were then accelerated by applying a negative potential difference on the filament relative to the chamber. Because of the electric field, the emitted thermionic electrons accelerated towards the chamber and collided with helium atoms in the process. The light excitations of the helium atoms produced characteristic blue illuminations. Initially, when the tungsten filament was exposed, the incandescent light from the filament was too intense to observe the helium illuminations. Hence, the design was improved by covering the filament with an aluminum foil coated ceramic tube to block the incandescent light.

Magnetic wire coils located around arms of the chamber produced magnetic fields. Using these coils, it was possible to apply magnetic fields similar to the Helmholtz configuration of strength around 8 G at the axial center. The filament had an electrical resistance of ~ 0.4 Ohms and the current of 1 – 2 A was needed to heat the filament enough to obtain the visible electron beam. The potential difference between the filament and the chamber was set to 160 V. As the surrounding wall heated the filament, internal pressure steadily increased from its initial at 50 mTorr. The measurements were carried until the pressure reached 500 mTorr, at which point the chamber was pumped out again.

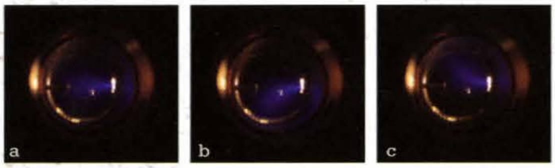

FIGURE 3
Electron beam illuminations at 250 mTorr helium, 150 eV. a, with no magnetic field, the beam trajectory is straight. With magnetic field of 8 G out of (b) and in to (c) the page, the beam bends showing a general single electron

LIGHTING IT UP

At 250 mTorr pressure and 150 V for the accelerating voltage, the distinct blue electron beam trajectory lasting 5 – 6 cm could be observed [Figure 3]. Additionally, by applying the magnetic field in the directions into and out of the page, the electron beam bent, showing the direction of the Lorentz force. Furthermore, varying the strength of the magnetic field changes the curvatures of the electron beam bending. When the beam is present, the thermionic currents between the chamber wall and the filament were measured as in the regions between 10 – 50 μA.

After the first set of the experiments, the design of the electron gun was improved so that the electron beam can be accelerated before it leaves the gun unit. This could eliminate the strong electric fields outside the electron gun, making that the magnetic effect dominate outside the electrongun. In addition, the helical trajectory of the beam would be more apparent if the beam path is longer and the chamber is large enough to adopt various magnetic field configurations. A larger chamber would make the pressure more stable, as the walls are further away from the filament and the filament heating effect is less noticeable.

The design also had to be altered to prevent degradation of the filament. As the thin filament was driven to very high temperatures, the filament started to disintegrate, especially when oxygen was present. Eventually the filament snapped in response to high enough temperatures, similar to the case of general incandescent bulbs. To adjust for this, the filament was connected to the electrode via spark-welding. Spark-welding was chosen since use of solder is not recommended in vacuum conditions, and this restricted attaching a thicker filament. The stability of the filament has now been improved by attaching a pre-made iridium filament.

There are other complications that arise from this design which were not as easily fixed. Computer simulation suggests that having a magnetic mirror field configuration in front of the filament could help in collimating the beam. However, this needs to be conducted at the electric field-free region. In addition, the effect of the magnetic field that could be applied in this setup is very weak compared to the effect from the electric field present in the chamber. This indicates that the bent trajectories of the beams in previous figures are influenced by both magnetic fields and electric fields. In order to achieve the magnetic field visualization by the helical trajectory of the electron beam, it is necessary to have the center of the chamber free from any electric fields.

When the region becomes free from the electric field, the electron beam will follow the lines of the magnetic fields with its Larmor radius. For 100 eV electrons, the Larmor radius can be made small with relatively weak magnetic fields of a few tens of Gauss.

MOVING FORWARD

In this experiment, it was shown that the electron beam could be visualized in a low pressure helium gas system by light excitations. The beam also aligns with the lines of magnetic fields, providing a possibility of imaging the vacuum magnetic field. Improvements to this design which would help in visualizing the magnetic field are to have a larger chamber that sustains more stable and lower pressures, apply stronger magnetic fields, and employ more durable filament designs in order to decrease the Larmor radius enough that the magnetic field lines are better aligned. Using computer simulations would also allow for estimation of the path of the electron beam at a known magnetic field structure. □

ACKNOWLEDGEMENTS

This work was supported by Summer Undergraduate Research Fellowship at Caltech as an exchange scheme between Caltech and Cambridge. I would like to thank Professor P. M. Bellan and members of his group for accepting me as a part of the group and their kind help throughout.

FURTHER READING

1. Bellan, P. M. Simulating Solar Prominences in the Laboratory. American Scientist 88, 136-143 (2000)

2. Electron charge to mass ratio experiment http://physics.ucsd.edu/was-sdphul/labs/2dl/exp4/exp4-THE.html, UCSD

3. Bellan, P. M. Fundamentals of Plasma Physics, 19 (CUP)

4. Stenzel R. L. Electron beam experiments. http://www.physics.ucla.edu/plasma-exp/beam/, UCLA

ADDITIONAL SUGGESTIONS

R. L. Stenzel at University of California, Los Angeles Physics department has built a powerful electron gun and carried out a number of electron beam experiments with different electric and magnetic configurations. His research page on the UCLA website contains many interesting photos of electron beam illuminations.

Mapping the Effects of Hallucinogens in the Mouse Brain

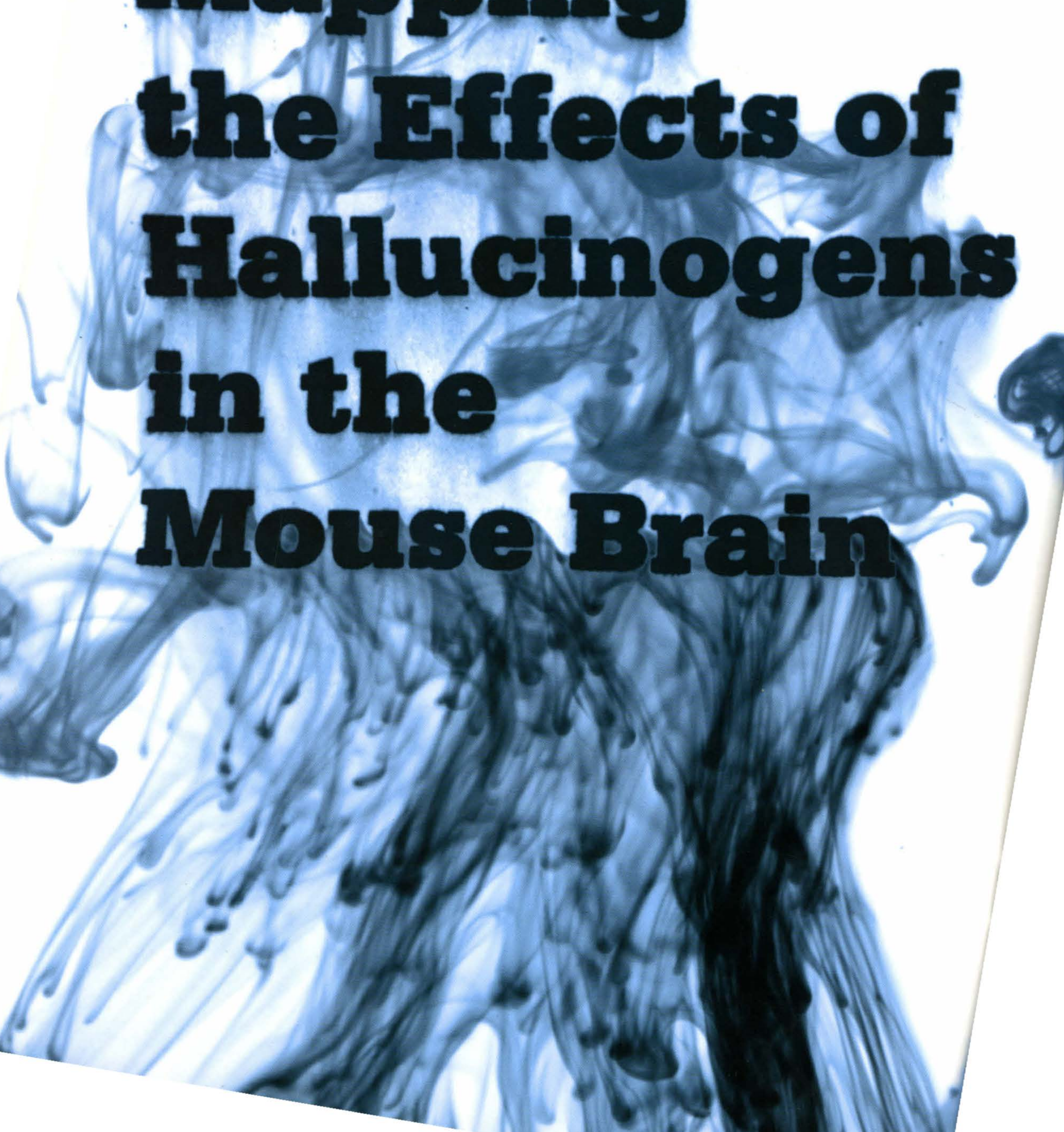

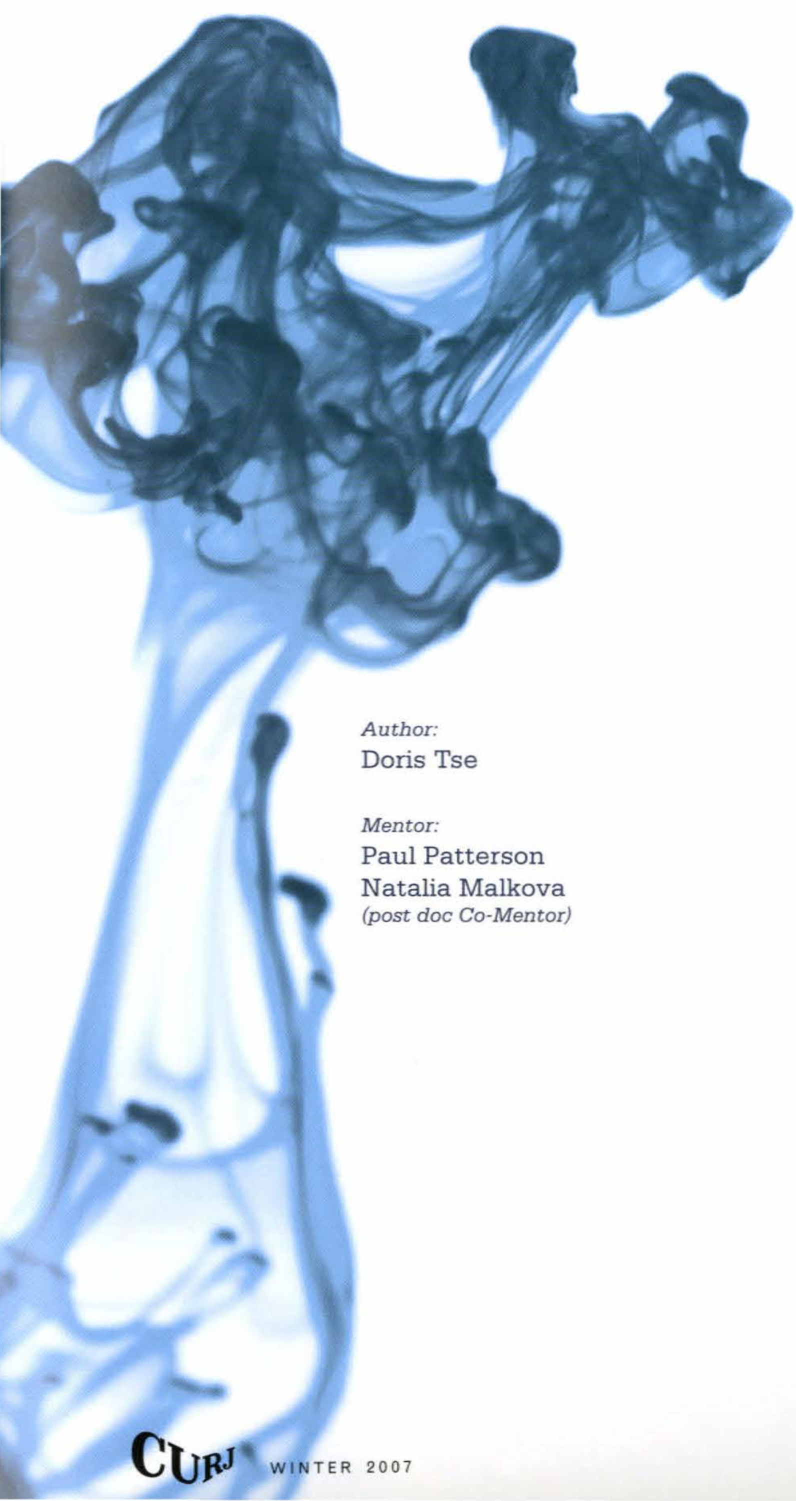

Author:
Doris Tse

Mentor:
Paul Patterson
Natalia Malkova
(post doc Co-Mentor)

THE HUMAN BRAIN REMAINS ONE OF THE GREATEST mysteries in modern science. From the mechanism by which the brain coordinates many complicated processes to the myriad of potential disruptions of normal brain function, the mind presents an intriguing puzzle, one that is yet to be completely assembled. As scientists uncover more details and shed light on specific brain activities, it has become clear that there are many more intricacies of the human brain waiting to be unraveled.

Mental illnesses in particular have been difficult for society and scientists alike to deal with. Ancient cultures labeled those with hallucinations and other mental diseases as socially unacceptable while modern society attempts to accommodate such individuals with specially tailored mental hospitals. Scientists have encountered difficulty in studying such disorders in depth due to both the complexity of the human brain and relative difficulty of investigating such illnesses. A particularly striking mental condition is Schizophrenia. Popularized in modern society through the story of the Nobel Prize winning mathematician John Nash in A Beautiful Mind, the exact causes and sites of abnormality in this mental illness are yet unclear. A potential solution can be found by turning to animal models of hallucination in an effort to determine the specific changes that can force minds to madness.

STRUGGLING WITH SCHIZOPHRENIA

Schizophrenia is a devastating mental disorder that affects one percent of the population worldwide with more than 2 million Americans suffering from the illness in a given year. Symptom severity is long-lasting, causing a high degree of disability and a significant incidence of suicide. Afflicted individuals experience positive symptoms, such as hallucinations, delusions, thought disorder, and altered sense of self, as well as negative symptoms including apathy, blunted feelings, depression and social withdrawal. Lewis and Levitt found that these clinical features typically appear in the late twenties and thirties, with the average age of onset generally about five years earlier in males than in females (Lewis & Levitt 2002). In 1996, U.S. mental health officials estimated that schizophrenia consumed $65 billion a year in direct treatment, societal and family costs. Therefore, it is becoming increasingly important that the causes of this mental illness are specifically mapped in order for more efficient treatments to be formulated.

Although researchers have identified several genes that are associated with an increased vulnerability to schizophrenia, Lewis and Levitt also found that a combination of genetic susceptibility and environmental perturbation appears to be necessary for the expression of schizophrenia (Lewis & Levitt 2002). Epidemiological studies have implicated severe maternal malnutrition, exposure to

"Brown discovered that respiratory infection during the second trimester raises the risk of schizophrenia in the offspring 3 to 7 fold..."

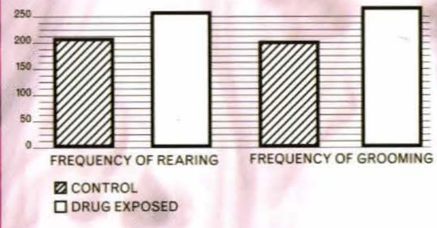

FIGURE 1
The hallucinogen DOI increases rearing and grooming activities in mice, when compared to control mice (no DOI injected).

influenza virus, birth in winter/spring months, birth in an urban area, repeated psychological stress, obstetrical complications (hypoxia/ischemia) and exposure to adverse intrauterine events as environmental risk factors (Boog 2004; Rantakallio P, Jones P, Moring J, et al. 1997; Radeler TJ, Knable MB, Weinberger DR 1998).

EXPLORING MATERNAL MECHANISMS AND TRACKING HALLUCINATIONS IN MICE

The most complete study of an environmental risk factor involves maternal infection. Brown discovered that respiratory infection during the second trimester raises the risk of schizophrenia in the offspring 3 to 7 fold (Brown, 2004). More recent studies have shown that the maternal response is to infection, rather than the virus itself. Support for this theory has come from studies reporting neurochemical and behavioral abnormalities in the offspring of mice injected with polyriboinosinic-polyribocytidilic acid (poly (I:C)). Poly-(I:C) is a synthetic double-stranded RNA, the precursor to DNA, that is used to mimic viral exposure. This RNA strand elicits an inflammatory response similar to that observed during viral infection in the mother without the use of an infectious virus.

Using this maternal immune activation model, the positive symptoms of schizophrenia were explored in mice. The goal was to determine whether mice can be shown to exhibit hallucinations and to then map these hallucinations to the expression of specific immediate early genes (IEGs). A "hallucination" is defined as the activation of the visual or auditory system in the absence of appropriate sensory input, which can be stimulated by known hallucinogenic chemicals such as LSD and DOI. Activation of 5-hydroxytryptamine 2A receptors (5-HT2ARs) plays a key role in the actions of these hallucinogens in humans; for example, LSD stimulates 5-HT2AR-dependent head twitch behaviors in mice. Moreover, DOI and LSD create profiles of gene expression in the brain that are not observed with related, non-hallucinogenic chemicals. It has also been shown by Farivar that levels of certain IEGs, such as c-fos, increase in all areas of the brain examined in response to acute LSD; this rapid up-regulation following neural stimulation has resulted in the extensive use of IEGs in functional mapping studies. (Farivar et al., 2004). To induce maternal immune activation, poly(I:C) was dissolved in PBS and injected into pregnant females on day nine of pregnancy. Plain PBS was injected in control animals. Offspring born to these poly (I:C) or PBS-injected mothers were then injected with varying concentrations of the hallucinogen DOI. A total of ten male mice were studied after being born in this manner.

The responses to DOI were measured in both control mice (PBS-injected mothers) and the offspring of mothers with activated immune systems via poly(I:C) injection. Behavioral responses to DOI were measured using an open field test in a translucent plastic box. In the open-field test, mice are placed individually near the center of the box, and their movements are followed by videotaping over a ten minute period. In these particular experiments, following the injection of DOI, mice were videotaped for thirty minutes. Total distance of travel, immobility, strong mobility (changing body position more than 90 degrees), and velocity (distance moved per unit time) were recorded. To test for hallucinogen-induced behavior, naïve animals were

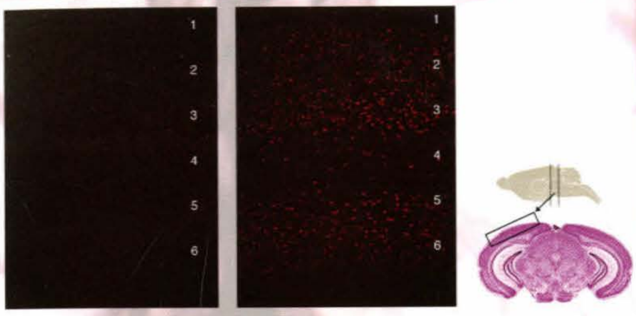

Control Drug Exposed

FIGURE 2 - Visual
The red box indicates the location of the visual cortex in a cross section of the brain. The bright red, prominent in the DOI exposed brain, reflects activation of Egr-1 in layers 2, 3, and 6 of the visual cortex. The control brain has little activation of Egr-1 in any layers of the visual cortex.

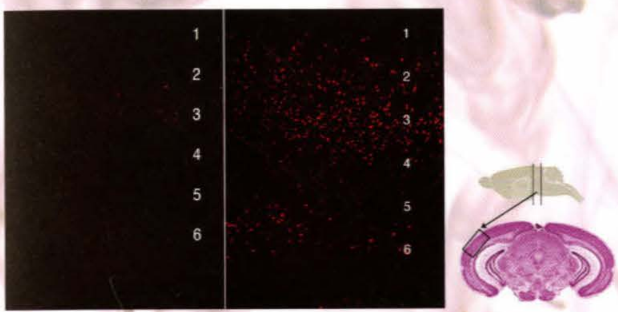

Control Drug Exposed

FIGURE 3 - Auditory
The red box indicates the location of the auditory cortex in a cross section of the brain. The bright red, prominent in the DOI exposed brain, reflects activation of Egr-1 in layers 2, 3, and 6 of the auditory cortex. The control brain has little activation of Egr-1 in any layers of the auditory cortex.

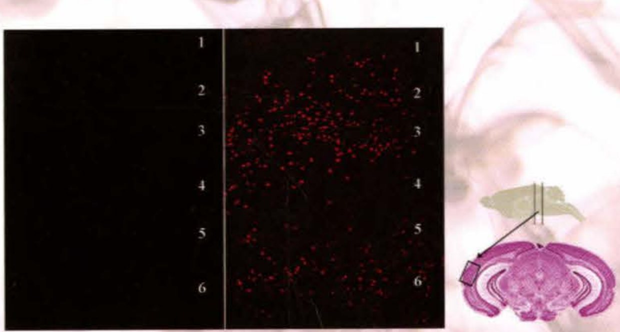

Control Drug Exposed

FIGURE 4 - Somatosensory
The red box indicates the location of the somatosensorycortex in a cross section of the brain. The bright red, prominent in the DOI exposed brain, reflects activation of Egr-1 in layers 2, 3, and 6 of the somatosensory cortex. The control brain has little activation of Egr-1 in any layers of the somatosensory cortex.

first habituated to red light in the testing room. After drug administration, rearing on hind legs and grooming frequencies were counted manually in real time. In addition, rearing and grooming frequencies were counted manually from the open field videos by observers blind to the experimental group of the mice, meaning they were unaware which group was experimental and which group was the control. Grooming behaviors for the mice involved standing on hind legs or washing the face/body.

Our results indicate that hallucinogen DOI seems to increase grooming and rearing activities in naïve mice, as exhibited by DOI-induced locomotion [Figure 1] and velocity changes. While we observe mice treated with a higher dose of DOI appear to exhibit higher grooming and rearing activities, more animals must be tested before the significance of the differences can be evaluated.

GAUGING GENE EXPRESSION

Gene expression in both PBS and poly(I:C) injected mice was studied utilizing immunohistochemistry of brains prepared through cardiac perfusion. Cardiac perfusion is a fast and efficient way to fix brain tissue. The animal is put to sleep, and a fixative solution is introduced into the heart under pressure. Fixative solution flows via the blood circulatory system throughout the mouse and rapidly fixes tissue. This fixation is necessary to stabilize the proteins in the brain in order to allow for antibodies to bind the proteins in immunohistochemistry, which allows analysis and identification based on the binding of antibodies to specific components of the cell. This labelling can subsequently be used to determine the expression levels of genes.

Our results indicate DOI enhances egr-1 expression in the visual, auditory and somatosensory cortices. Injection of DOI in the dark increases the immunostaining for egr-1 in layers 2, 3 and 6 of the visual, auditory and somatosensory cortices. In contrast, injection of PBS does not alter basal egr-1 staining [Figures 2-4]. No DOI-induced increase in staining was observed in other brain

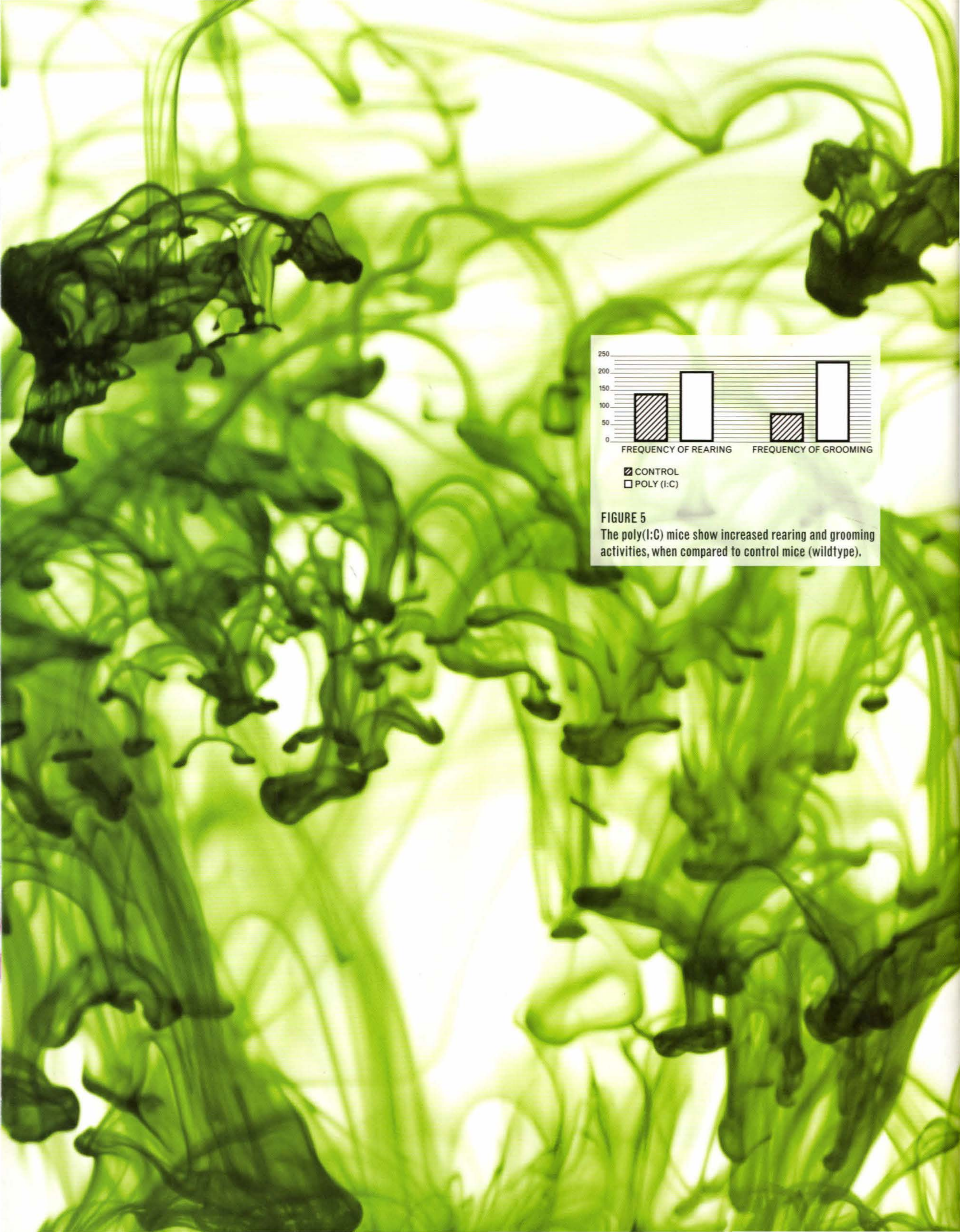

FIGURE 5
The poly(I:C) mice show increased rearing and grooming activities, when compared to control mice (wildtype).

areas examined (hippocampus, striatum, thalamus, amygdala) except for motor cortex. These results indicate that DOI stimulates IEG expression in auditory, visual and somatosensory cortices, as well as in the central nucleus of the amygdala. This stimulation is highly selective, as expression is not detected in any other brain area visualized in the same sections. Although there are structural differences between mouse brains and human brains, the homologous primary visual and auditory areas are well established. Thus, the pattern of activation is consistent with that expected for auditory, visual and somatosensory hallucinations.

AN INTRIGUING CONTRAST

Since the DOI stimulates expression of several IEGs specifically in brain areas appropriate for hallucinations, we wanted to determine if offspring of immune-stimulated mothers are more sensitive than controls to DOI. To optimize potential differences in such an experiment, it was necessary to determine what a sub-threshold dose of DOI would be. A sub-threshold dose of DOI is a minimal dose of the drug that induces stereotyped behavior in mice compared to saline-treated animals. The dose-response relationship for stimulation of grooming reveals that 0.1 mg/kg is a sub-threshold dose.In these preliminary data, the offspring of immune-stimulated mothers (injected with poly(I:C)) display a higher frequency of rearing than controls under both open-field and red light, home cage conditions [Figure 5]. They also show a greater distance of travel, total duration of strong mobility, and velocity while exhibiting a lower total duration of immobility. Therefore, mice born to poly(I:C)-treated mothers seem to their motor behaviors stimulated to a greater degree than controls by DOI, revealing they are more susceptible to developing hallucinations.

PRACTICAL APPLICATIONS

It is often said that schizophrenia is a uniquely human disorder because the positive symptoms of hallucinations and delusions are not detected in animals. However, the histochemical and behavioral data presented here suggests that this animal model exhibits a diagnostic, positive symptom of schizophrenia. Further studies could test hallucinogen-like changes in neuronal activity using fMRI, which would provide a more direct comparison with the human schizophrenia studies and clinically applicable information. Furthermore, auditory hallucinations are reported by 50 to 70% of schizophrenia patients, and they are often associated with acts of violence and suicide. Since the cause for this correlation is unknown, an appropriate animal model could be useful in exploring pathogenesis as well as novel therapeutic avenues in humans, both of which could help illuminate the mystery surrounding this disorder. ☐

ACKNOWLEDGEMENTS

I would like to thank Professor Paul Patterson, Dr. Natalia Malkova, Dr. Bobbi Carlson, Limin Shi & Jan Ko, Andrew Wang, Dr. Yi Zhao, Douglas Muhlestein, and the Patterson Lab. Furthermore, I would like to acknowledge the Student-Factuly Programs Office and the Summer Undergraduate Research Fellowship sponsored by Caltech for this opportunity.

FURTHER READING

1. Lewis DA, Levitt P. Schizophrenia as a disorder of neurodevelopment. Annu Rev Neurosci. 2002; 25:409-32. Epub 2002 Mar 22. Review

2. Boog G. Obstetrical complications and subsequent schizophrenia in adolescent and young adult offsprings: is there a relationship? Eur J Obstet Gynecol Reprod Biol. 2004 Jun 15;114(2):130-6. Review.

3. Brown AS, Begg MD, Gravenstein S, Schaefer CA, Wyatt RJ, Bresnahan M, Babulas VP, Susser ES. Serologic evidence of prenatal influenza in the etiology of schizophrenia. Arch Gen Psychiatry. 2004 Aug;61(8):774-80.

4. Farivar R, Zangenehpour S, Chaudhuri A. Cellular-resolution activity mapping of the brain using immediate-early gene expression. Front Biosci.2004 Jan 1;9:104-9. Review.

DESIGN AS RESEARCH

Introduction by Shawn Randall
Design Commentary by Dan Forbes
Conclusion by Helen Lee

INTRODUCTION

AS A DEPARTURE FROM PAST ISSUES OF THE CURJ, which were mostly computer rendered and fairly traditional, information design pieces, this year's magazine designer, Dan Forbes, was encouraged to explore and experiment in a similar fashion to the undergraduate scientists who wrote each article. Dan conducted preliminary research, gathered information related to the articles themselves and then brainstormed and planned a series of physical experiments to explore core concepts. Each experience allowed Dan to empathize with the authors and clarify the key ideas in his own head. These experiences are manifest throughout this issue as visual and physical artifacts. In a way, Dan was employing empathic methods of research to gain insights and also provide a new level of tactility that ultimately emphasized the process that scientists go through to learn and uncover new knowledge. Through this process, he in turn learned about the principles in question and created an interesting dialogue between concept and artifact.

DESIGN COMMENTARY

I TOOK ON THIS PROJECT BECAUSE IT MADE ME uncomfortable. Designing this magazine was incredibly intimidating because I hadn't ever worked with so much copy and with so many topics that I knew nothing about. I had to completely rely on the editors to explain the basic scientific concepts behind each of these in depth research projects so that I might be able to interpret them correctly.

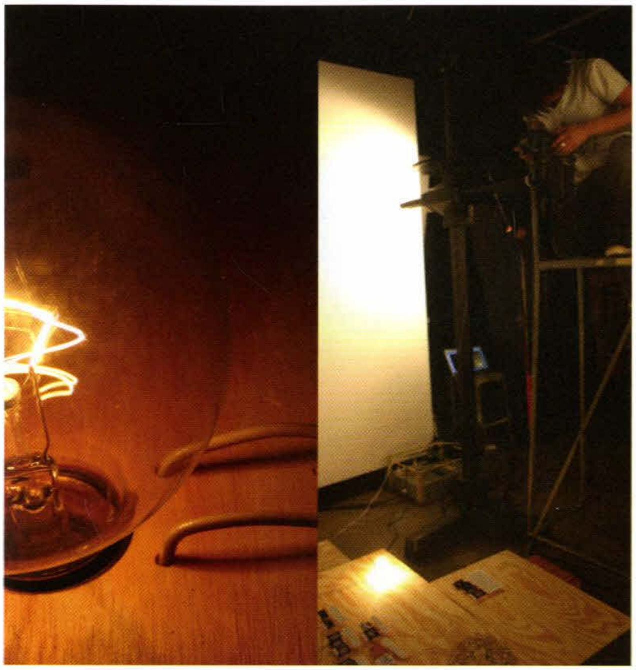

TRACING CONNECTIONS IN THE GORILLA BRAIN

This research project excited me when I learned about a potential visual difference in the map of connections in the brain of a musician and a non-musician. After analyzing each image from the article, I was particularly interested in the anisotropy image of a cross-section of the gorilla brain. Since our brains are made up of connections where this article specifically involved creating a map of the connections in the brain, I created 3 brain-like mazes. An idea that these brain mazes could become physical objects and photographed came up in my discussions with Shawn, our graphics advisor. In the end, I decided to string wire around nails that were in a sheet of plywood where the three brain mazes were then strung together and connected to a glowing light bulb near the end. Yusuke Nishimura digitally photographed it.

MEASURING THE PHASE OF LIGHT

The first experiment I conducted was to create a stereoscopic image. (Two photographs taken with a stereoscopic camera. One photograph represents the left eye, and the other the right eye. When the two photographs are viewed together, they combine to create a single image with depth and relief.) I felt this was appropriate because this new method made it possible to see something that was always there, but invisible to us. As I continued to explore this idea I found several difficulties because not everyone who sees the article will be able to see the image I wanted to convey. So I started over. I conducted a few experiments with transparency and light. Projecting light through printed transparencies. But again, failure. I began thinking about the breakdown of white light to fundamental colors when traveling through glass. With that in mind I laser-cut clear acrylic and put it onto a light table to closely photograph it. The finished piece was quite similar to the device which the article talks about: using light to define a transparent object to create form and spatial relationships.

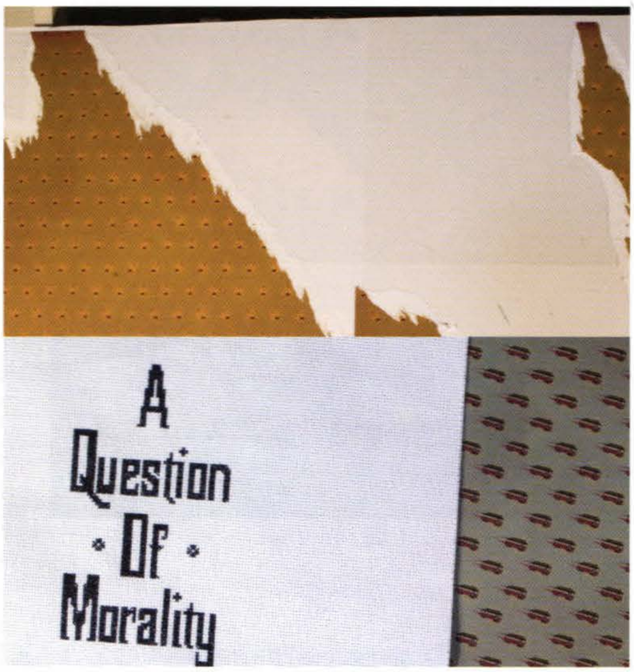

A QUESTION OF MORALITY

I felt that this article could be viewed as perhaps a series of images of different layers of wallpaper as this article dealt with the multiple complex layers of morality.The idea of home and family gave me all of the inspirations for using wallpaper and cross stitching in the design. I created a cross-stitched pattern that would eventually be utilized as the title of the article. It was graciously stitched by Sarah Prieto, a good friend of mine. I continued to create icons and later patterns of a speeding trolly and a train track switch that would become the wallpaper used in the backgrounds of these articles.

SEEING MAGNETIC FIELDS

The design itself was very literal; it was about finding methods to visualize magnetic fields. I laser-cut thin automobile magnets into related illustrations and placed the magnet beneath a clean sheet. I then sprinkled metal filings on top of the sheet. The magnet grabbed the filings and aligned them to the different shapes of the magnet fields caused by the shaped magnets. The article layout itself is made up of the photographs of this experiment.

MAPPING THE EFFECTS OF HALLUCINOGENS IN THE MOUSE BRAIN

If you've ever gazed at cloudy skies, you know what it feels like to see the clouds take shape of random familiar objects and shapes. The graphics of this article are much like looking for pictures in the clouds. Essentially there is nothing there but the clouds allowing you to shape what you see into what you want to see. To accomplish this effect, I dropped neon food coloring into an aquarium and digitally photographed the result.

CONCLUSION

ONE OF THE STRENGTHS OF THE CALTECH Undergraduate Research Journal is being able to bring together both art and science into one medium. These two fields are not mutually independent but really bits and pieces of the other as our magazine continually displays. And it is our pleasure to present to you, the reading audience, with the first CURJ issue where the layouts themselves were a part of an ongoing experiment and true display of the fusion of art and science. □